Hardware Design and Evaluation of Non-planar Fused Deposition Modeling on a 3-axis printer

Samuel Bengtsson

DIVISION OF PRODUCT DEVELOPMENT | DEPARTMENT OF DESIGN SCIENCES
FACULTY OF ENGINEERING LTH | LUND UNIVERSITY
2023

MASTER THESIS

Hardware Design and Evaluation of Non-planar Fused Deposition Modeling on a 3-axis printer

Samuel Bengtsson

LUND UNIVERSITY

Hardware Design and Evaluation of Non-planar Fused Deposition Modeling on a 3-axis printer

Published by
Department of Design Sciences
Faculty of Engineering LTH, Lund University
P.O. Box 118, SE-221 00 Lund, Sweden

Subject: Technical Design (MMKM10)
Division: Product development
Supervisor: Jože Tavčar
Co-supervisor: Axel Nordin
Examiner: Per Kristav

Abstract

The technology of Fused Deposition Modeling (FDM) has been spreading quickly since the advent of low-price 3d-printers which enabled many more people to participate in the technology. As the use of it increases also does the needs of the people using it, with the addition of new features in the software, hardware or the study of what factors produce the best print results. This has enabled the concerted effort of many to produce a rapid development in what FDM can be used for. The uses can range from printing small models, fixing things around the house to complex prototypes. These separate interests also have separate goals for what their prints should achieve such as high fidelity, good strength, or maybe fast print times when doing repeated iterations.

To further the continual improvement of FDM this thesis took steps to examine a non-planar FDM approach based on its ability to produce higher quality results in surface finish. This was done through modification of the hardware of a consumer 3-axis FDM printer combined with new software available for non-planar slicing. The goal was to establish the most influential combinations of hardware and software factors through Design of Experiments methodology. A novel way of measuring surface finish was used, and its viability analysed. The results from the work showed that the nozzle design played a major part in the non-planar printed parts surface quality with a less dominant impact from surface fill of the top surfaces and the nozzle temperature. Future avenues of research will also be discussed stemming from the gathered results.

Keywords: Non-planar Fused Deposition Modelling, Additive Manufacturing, Design of Experiments, Nozzle design

Sammanfattning

Tekniken för Fused Deposition Modeling (FDM) har spridit sig snabbt sedan tillkomsten av lågpris 3d-skrivare som gjorde det möjligt för många fler människor att delta i tekniken. När användningen av teknologin ökar, ökar också behoven hos de personer som använder den, med tillägg av förbättringar i mjukvara, hårdvara eller optimering av processfaktorer tänjs gränserna för FDM:s möjligheter. Detta har gjort det möjligt för mångas samlade ansträngning att driva på en snabb utveckling av vad FDM kan göra. Användningsområdena kan sträcka sig från att skriva ut små modeller, fixa saker runt huset till att skriva ut större komplexa prototyper. Dessa separata intressen har också separata mål för vad deras utskrifter ska uppnå, såsom hög kvalitet, bra styrka eller kanske snabba utskriftstider när de gör upprepade iterationer.

För att främja den ständiga förbättringen av FDM undersöker denna avhandling en icke-plan FDM-teknik, och dess förmåga att producera utskrifter med bra resultat i form av högre kvalitet i ytfinish. Detta utfördes genom modifiering av hårdvaran i en 3-axlig FDM-skrivare i konsumentklass kombinerat med en ny mjukvara tillgänglig för icke-plan slicing. Målet var att etablera de mest inflytelserika kombinationerna av hårdvaru- och mjukvarufaktorer genom Design of Experiments-metodologin för att utröna signifikanta faktorer. Ett nytt sätt att mäta ytfinish presenteras även och dess gångbarhet utvärderas. Resultaten från arbetet visar den stora roll munstyckets design har på ytkvalitén för utskrifter i icke-plan FDM, samt den mindre rollen av topyteorienting och temperatur. Framtida forskningsvägar diskuterades även för icke-plan FDM.

Nyckelord: additiv tillverkning, munstyckedesign, icke-plan Fused Deposition Modeling, Design of experiments

Table Of Contents

1 Introduction

1.1 Background

Non-planar Fused Deposition modeling as a concept has been around for a long time (2008) but only recently has seen deployment of software solutions allowing for wider use (2022) (2018). A development area has been the attempts to generate and run machine code which makes greater use of the additional axis of movement a printer might have to achieve certain results. This takes its form by printing non-planar layers, meaning non-flat, which contrast to conventional methods of FDM which in most cases only create flat cross sections of the printed model upon each other until completion while holding on movement axis almost still. The traditional FDM technology is simple and there exists a lot of stable software available to produce 3d prints in this way. But there are several reasons to pursue a non-planar approach to this: achieving greater strength, surface finish or to diminish the need for support material, among other things.

When looking at non-planar FDM there are a lot of uncertainties, most FDM printers are unsuited for using the technology, the software that exists for its use is not widely used or developed by large companies. The level of development is still at a research stage compared to planar FDM, which makes it an interesting area of study due to the many avenues of improvement available.

1.2 Purpose

This work aims to examine a promising software solution for non-planar FDM that enables generation of machine code for consumer FDM-printers and extend the knowledge of what needs to be modified in terms of hardware on a consumer grade printer to enable the greatest usage of CFDM features. Through Design of Experiments testing a measure of how the printer parameters affect the final result will be gathered as well as how capable a 3-axis FDM printer is of using this technology.

1.3 Delimitations

FDM is useful for many things, therefore it was decided to limit the scope of the project to the analysis of CFDM for its ability to create better surfaces quality than FDM. While other effect gains such as strength gain and print time could be considerable this work will solely focus on the potential effect improvements on the surface finish of CFDM printed parts.

As the field of CFDM is a new area of research it will require an approach to the measure of surface finish for a non-planar printed part which has not been previously documented. While terms such as stair stepping and over extrusion are still applicable the area comes with several new unique surface defects to the technology that will need to be analysed. Stemming from this the analysis will be based on prior experience of FDM as well as the results of the samples produced with CFDM.

1.4 Approach

The project was divided in three parts: the modification of the printer, testing of non-planar printing for impactful parameters, and finally experimentation of these parameters' interactions and combined impacts through a design of experiments test.

The required changes to the hardware used prior research in non-planar FDM combined with findings from practical tests to determine the issues with the current design and what level of modification would be necessary for the tests.

The testing procedure involves testing the capabilities of each modified component in regard to each specific function. The cooling performance of the fan shroud, the flow properties of the nozzle and the ability to reset the height probe. The software used for slicing the models will also be explored to identify within which limits the process parameters of printing can safely be varied.

Following this a design of experiments (DOE) approach will be applied to determine the impact of process parameters and hardware modifications, as well as their interactions. The parameters used during the experiment will be determined from previous work in the area of non-planar FDM and results from prior component testing. The measurements will use a novel approach to measure surface defects. Finally, the measurement results will be compiled into graphs and evaluated for their statistical significance.

2 Literature review

A description of the technology of additive manufacturing as well as some specific developments in the field of non-planar fused deposition modelling will be described in greater detail. As well as the necessary background of the modifications made to the printer.

2.1 Additive Manufacturing

Additive manufacturing (AM) can generally be explained as any production principle which builds a product up by added material contrary to traditional methods of manufacture which rely upon removing material from a base object to achieve the final shape (SME, 2022).
There are numerous technologies that employ AM depending on the intended result. From producing high quality prototypes to being used for complex parts for turbines or general use for home repair. This necessarily means that the approaches also vary greatly in material used, software and complexity of the system used.

2.1.1 **Use of AM**

From prototyping to making real usable parts, AM has become an increasingly useful tool in the product development process. It has gone from relatively crude recreations of computer models to being used to manufacture precise parts in industries for use with aerospace, automobiles, and production tools integrated with other manufacturing processes (Autonomous Manufacturing, 2023).

The AM process allows for a faster time from design to receiving a product, but this must be balanced with the longer time to produce a single part compared to, for example, extrusion moulding or forging if it is to be used for larger scale manufacture. The relative newness of the implementation of AM machines in many industry also leaves a gap of experience for the process knowledge necessary to run these machines efficiently, safely and with good result. The development of new software and higher performing machines will allow for more widespread use of

AM technology in industries where it currently would not be feasible due to the previously named issues.

2.1.2 **FDM (Fused Deposition modeling)**

FDM is a manufacturing method in which a filament of material is extruded from a nozzle to build up a model point by point to create a final object. A wide range of materials are available such as plastics, clay, or even food materials such as chocolate, see Figure 2.1. The barrier for a material to be used in the FDM process can be said to be that it needs to be viscous enough to be extruded through a nozzle and then have properties that allow it to solidify after being deposited.

Figure 2.1 (Left) A FDM print in chocolate (Mycusini, u.d.). (Right) A pot printed in clay (3DPotter, 2023).

Since the expiration of patents related to FDM 14 years ago the ability for manufacturers to produce machines using the FDM technology was unlocked (3DSourced, 2021). This led to a large drop in price and an increase of the number of printers and printer kits directed at hobbyists (Filemon, 2016). Due to the large and growing userbase of FDM the technology has seen fast development in both software and hardware with faster machines driven by enthusiasts and increasing knowledge of the factors which dictate the final product appearance and its properties, be it the hardware design of a printer or changes to the software used for slicing.

A comparatively new development and the focus of this thesis has been the attempts to generate and run machines in a way which makes greater use of the movement capability of the different kinds of FDM printers by printing non-horizontal layers.

2.2 Non-planar FDM

Non-planar FDM (sometimes called Curved Fused Deposition Modelling, or CFDM), works similarly to conventional FDM in the way that the 3d printer used receive g-code commands and resolve these through movement from its axis. As the name implies the g-code generated consists at least partly of movements which are not constrained to strictly horizontal layers, which can be seen visualized in Figure 2.2B.

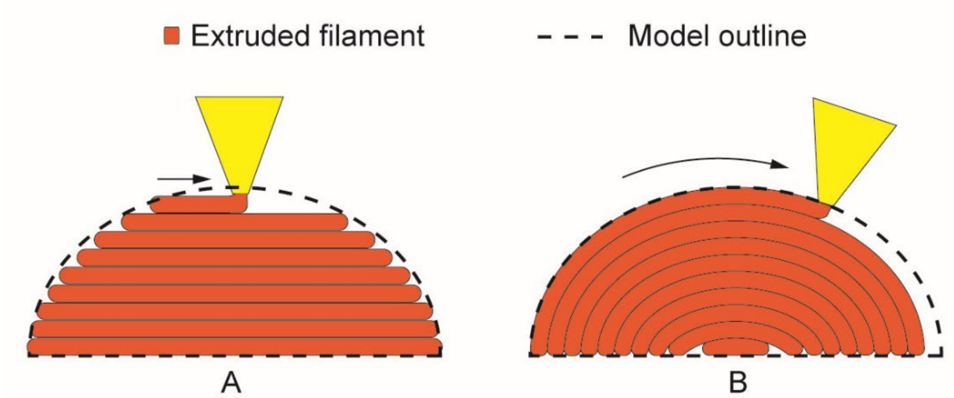

Figure 2.2 Schematic drawing of the difference while printing between conventional slicing (A) and non-planar slicing (B).

There are benefits to look further to the application of non-planar layers in FDM. When not limiting the travel in any direction of a printer would be enabling a more accurate reproduction of surfaces which otherwise would be subject to stair stepping. The inaccuracy that comes from the approximation of layers can be seen in Figure 2.3(left), where the individual layers are clearly visible. With a more even surface on the part which employed non-planar printing techniques in Figure 2.3(right). There are other benefits to print performance from developing non-planar FDM such as parts with greater strength, greater resolution parts and a reduced need for support material.

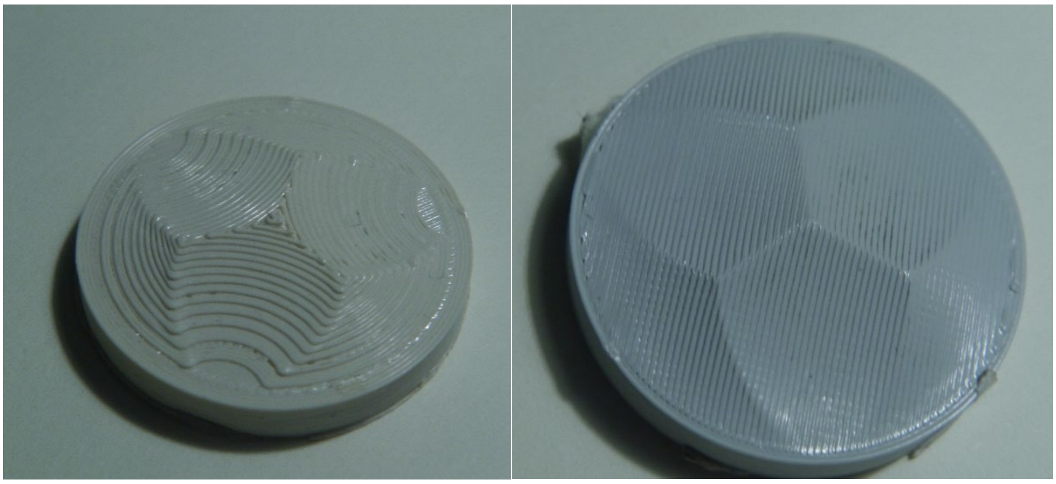

Figure 2.3 A part printed with conventional slicer settings showing stair-stepping artifacts(left), and a part printed with non-horizontal layers with less visible stair-stepping(right).

2.3 Different methods Achieving Non-Planar FDM

The most common method of FDM involves a machine capable of movement in three axis in a cartesian system. It is, however, not limited to such a system. FDM machines capable of movement in 4-axis and above have been tested for the purposes of CFDM. The advantage of the added movement directions is that greater clearance can be achieved to avoid collision with previously extruded material, see Figure 2.4A, as well as the nozzle applying more even pressure on the extrusion for better adherence to previous layer, see Figure 2.4.

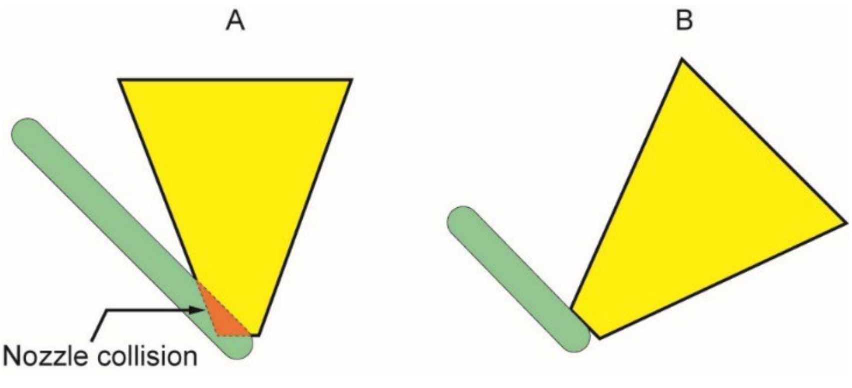

Figure 2.4 Nozzle colliding with extruded filament as printing angle gets higher.

2.3.1 **Printing of Complex Non-Planar Forms with a 6-axis system**

In a work by (Mitropoulou, Bernhard, & Dillenburger, Nonplanar 3D Printing of Bifurcating Forms, 2022) a non-planar printing solution was implemented to use a 6-axis robot arm for its operation, while only using 5 in the current work. The method expanded on a previous work from the same authors (Mitropoulou, Bernhard, & Dillenburger, 2020) to allow for better handling of branching models, see Figure 2.5a in which a system for segmenting has been used to indicate different printable areas. The operation of the robot arm and a printed prototype can be seen in Figure 2.5b and c.

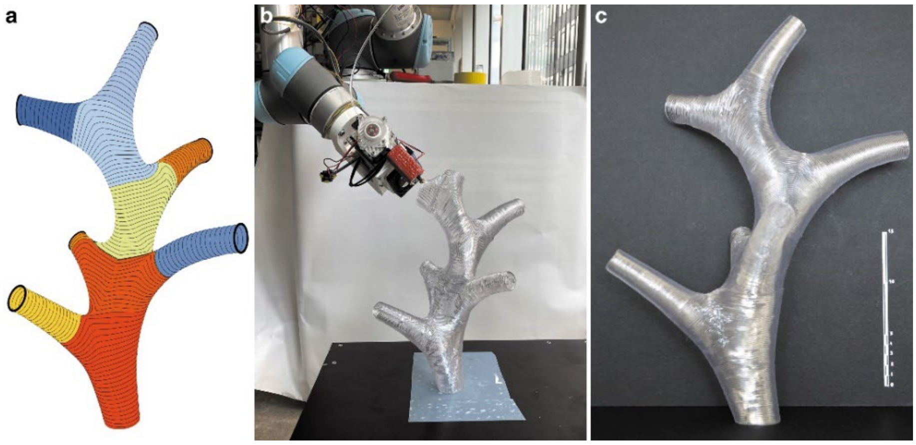

Figure 2.5 non-planar printing by robotic arm to create complex shapes, showing *a*, the segmentation of a model into areas which dictate the order of printing, *b* the printing of the model, and *c* the finished prototype. From (Mitropoulou, Bernhard, & Dillenburger, Nonplanar 3D Printing of Bifurcating Forms, 2022).

The report concluded that more geometrically complex models could be processed as compared to the previous work as well as showcasing the benefits of a CFDM approach as the prints did not need support material and had a more pleasing appearance due to the layer lines conforming to the shape of the model.

2.3.2 **Combination of Planar and Non-Planar Layers – a 3-axis Approach**

In a paper by (Ahlers, 2018) a slicer was modified so that machine code for the generation of hybrid planar and non-planar layer generation was possible for a given part. The software only uses non-planar layers to cap of a print by modifying the top surface infill and perimeters to follow the surface of the model more closely, the combination of planar and non-planar areas can be seen in Figure 2.6c and d. With a comparison of stair stepping made in Figure 2.6a and b for high and low layer heights respectively. The rest of the part prints conventionally in planar layers. This makes the usage of the technology suitable for many 3-axis printers with low clearance around the hot-end. Furthering this by allowing settings for an individual printer's clearance to be input in the software to warn the user of potential collisions or restricting the areas where non-planar printing is used to the printers' limitations.

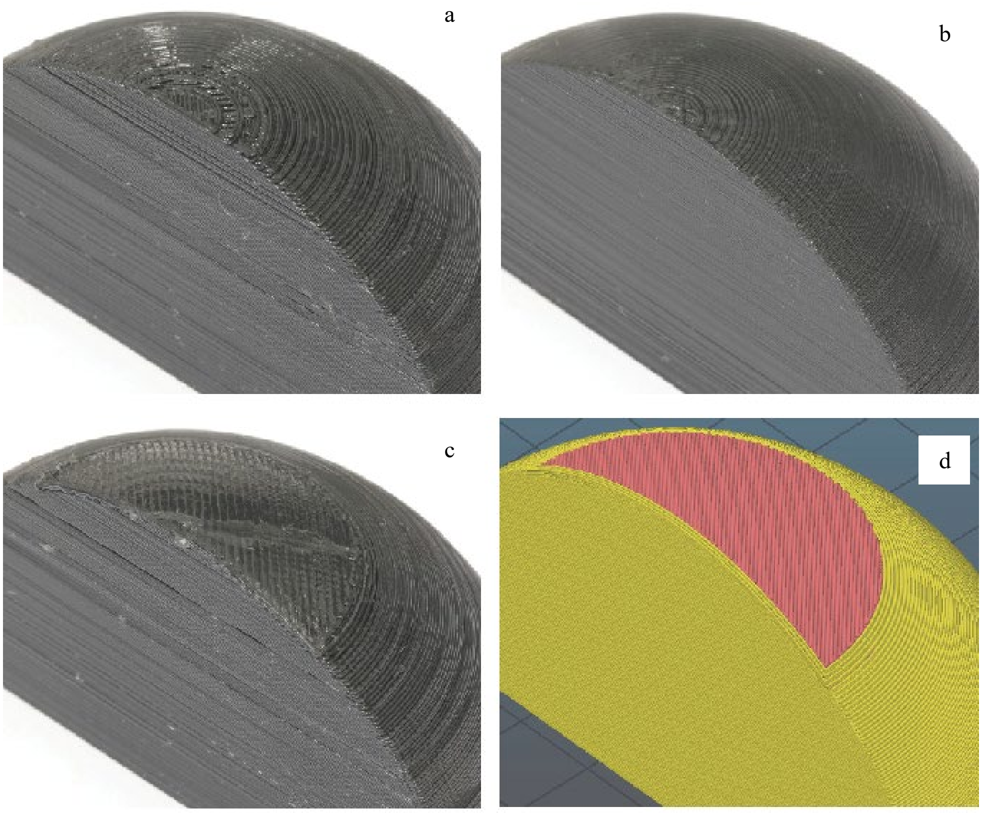

Figure 2.6 Comparison of surface appearance between a) large layer height b) low layer height c) large layer height combined with a non-planar top surface d) the slicer preview of c). Picture from (Ahlers, 2018).

2.3.3 **CFDM capable slicer software**

For the purpose of this thesis all non-planar models were generated with the slic3r version developed in (Ahlers, 2018). The software was used to generate all test files for the project. To use the software's non-planar layer function, values for the clearance around the hot end were inserted. This is used to detect any interference that could occur while printing from either the nozzle (which dictates maximum nonplanar angle) or the hot end, see Figure 2.7. The slicer allows for configuration of common planar printing parameters as well. Varying these parameters would be the basis for the process experiment along with the hardware changes.

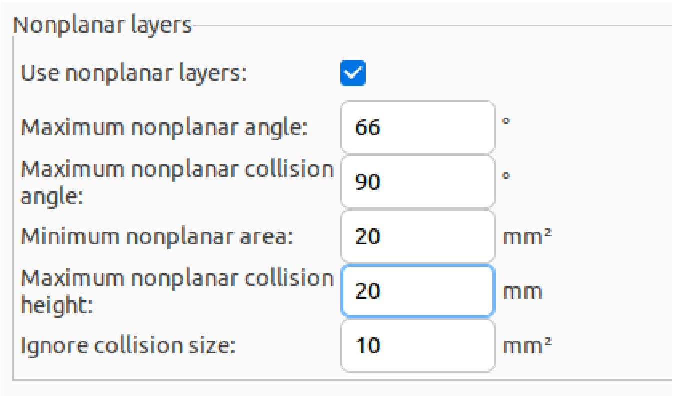

Figure 2.7 Settings for non-planar printing in the Slic3r version.

The preview of the g-code would then be shown before being exported to see if any irregularities could be found, such as the g-code preview in Figure 2.8.

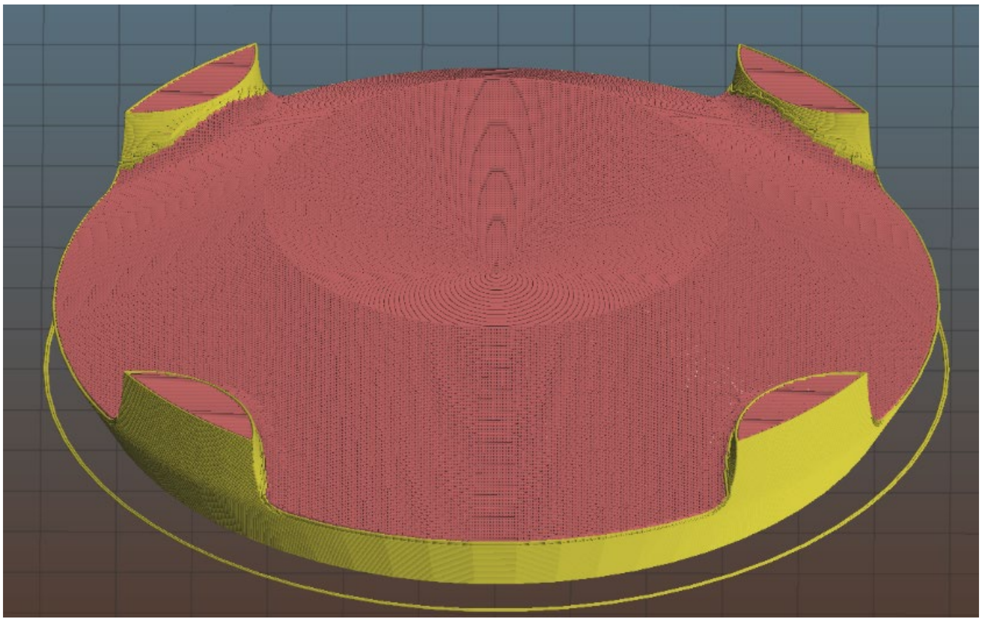

Figure 2.8 G-code preview with non-planar layers laid on top of the model combining into planar layers where the settings indicate that a collision would take place.

2.4 Hardware

2.4.1 **Nozzle design for CFDM**

For the printer to be able to produce greater angle non-planar surfaces the nozzles were made longer to extend further from the hot end of the printer, improving the clearance around it. Based upon the original drawing of the E3D nozzle (see appendix B.1 for full drawing (JoshuaRowley42, 2017)) one lengthened version with the same tip area as well as one with a reduced tip area were made. The reduced tip area was achieved by adding a secondary angle at the tip see Figure 2.9B. The standard size of 0.4mm was used for the nozzle orifice as it is a common size and balances speed of printing with quality. Two nozzles in total were produced to be tested in the analysis:

- A longer nozzle with an exposed length of 10mm, 5mm longer than the standard E3D nozzle (see Figure 2.9A).
- A longer nozzle with an exposed length of 10mm, as well as an added secondary angle at the tip which reduced the flat area at the tip from 1mm to 0,6mm in diameter (see Figure 2.9B). The purpose of this was to study the impact, seen in figure Figure 2.4, of the nozzle colliding with deposited plastic.

The geometry of the nozzle has an effect on the flow behaviour of the plastic being extruded. To make the comparison fair between the nozzles the following related printer setting were calibrated and adjusted per nozzle:

- Retraction – The amount of plastic that is retracted into the hot-end after a finished line to minimize excess plastic due to oozing (Prusa3D, 2022).
- Flow rate multiplier – controls the amount of plastic that is extruded, which can be adjusted if the flow of plastic has changed through the nozzle. Calibrated by measuring single wall thickness of a hollow form according to (Prusa3d, 2022).
- Linear advance – A factor used to correct for different pressure build up depending on the nozzle used. It works by changing the amount of filament that gets extruded through the nozzle when slowing down at the end of a line segment (Prusa 3D, 2022).

Machining of the nozzles was done on a manual metal lathe from brass hex stock. The order of operations for the machined nozzles were planned with the supervision of workshop personnel at the IKDC workshop.

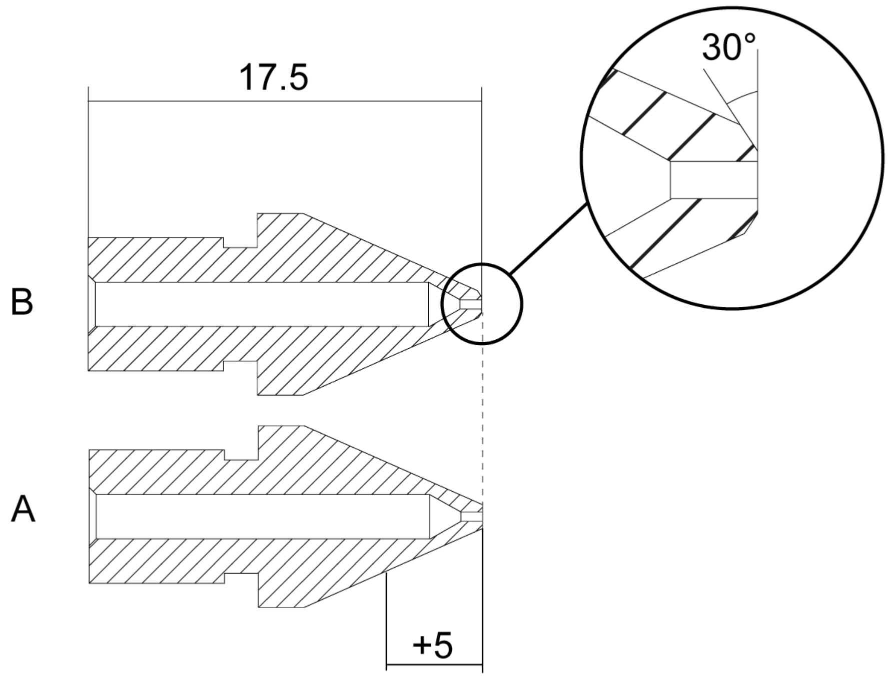

Figure 2.9 The changes made to the nozzle design. A and B were both extended by 5mm to a total length of 17,5mm compared to a length of 12,5mm for the E3D nozzle. The B nozzle was given a 30° angle at the tip.

The intention of the nozzle design was to make use of prior knowledge gathered in other works regarding non-planar printing where concerns regarding the nozzle geometry were raised.

2.4.2 **Non-planar FDM fan shroud**

In most machines made for 3-axis FDM-printing the fan shroud is made for printing horizontal layers upon each other, where no collision would be expected. Therefore, a new solution would need to account for the lower position of the extruder nozzle during printing to achieve acceptable cooling while moving it further away from the print operation. The impact of cooling on dimensional quality has previously been studied in (Lee & Liu, 2019), where the accuracy between a printed part (PLA plastic) and the nominal model dimensions saw improvement due to cooling. As this work aims to study surface quality, which has some common aspects to dimensional accuracy, the need for cooling was deemed important enough to implement a new fan shroud solution.

To create the design Solidworks 2021 (3ds.com) was used along with the flow simulation module where the fan performance curve for the standard print cooling fan was approximated with help from the Prusa3D printing support team. This data was necessary to find a comparable fan performance curve from a fan with similar specifications, see Figure 2.10.

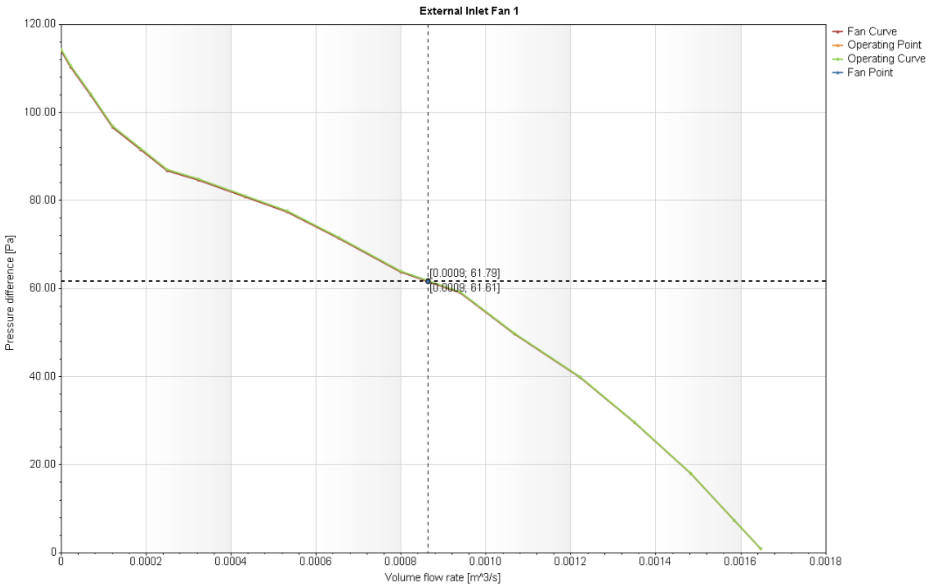

Figure 2.10 The operating curve for the blower fan used for simulations in theSolidworks flow project. Data taken from (Sunon, 2022, p. 190).

As thesis does not aim to compare different cooling solutions or the effect of a certain cooling solution over another the final result is only a draft of what a potential solution could look like for a CFDM system. Although tests of the effectiveness of the final design were ran to measure if the new fan shroud had at least as good cooling capacity as the standard fan shroud, while also being able to direct air towards the tip of the nozzle toward the extruded filament.

The modelling of the fan shroud used the existing extruder head geometry to create as close of a fit as possible for the new shroud and flow simulation tools available in Solidworks 2021 to check the effectiveness of a given solution. The software measures flow of air through the modelled fan shroud and determines the necessary static pressure to push the air through it. Leading to a value of volume air flow rate in the fan performance curve. The final fan shroud design aimed to be outside the stall region of the operating curve to minimize noise and risk for damage to the fan (Aerovent, 2018).

The performance of the new fan shroud was compared to the original design with an overhang test to benchmark its cooling capacity and was found to be suitable as it had comparable performance to the stock shroud when using a standard nozzle, see Figure 2.11. A test was also done without cooling in PLA. It failed due to curling of the plastic as can be seen in Figure 2.12, which shows the need for adequate cooling in PLA.

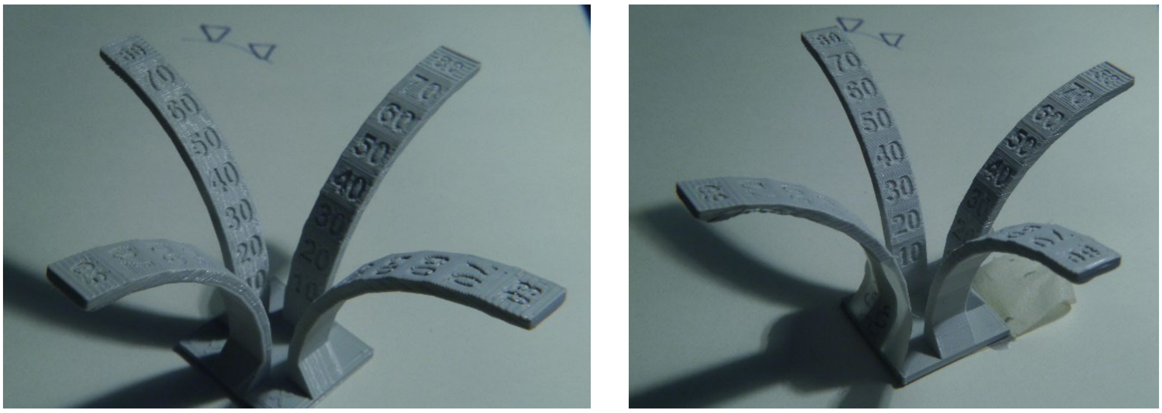

Figure 2.11 Left: result of overhang test with stock fan shroud and stock 0.4mm nozzle. Right: Result with fan shroud modified for CFDM.

In Figure 2.13 the simulation of flow from the CFDM fan shroud can be seen being directed mostly downwards toward the tip of the nozzle. The final version of the fan shroud can be seen in Figure 2.14.

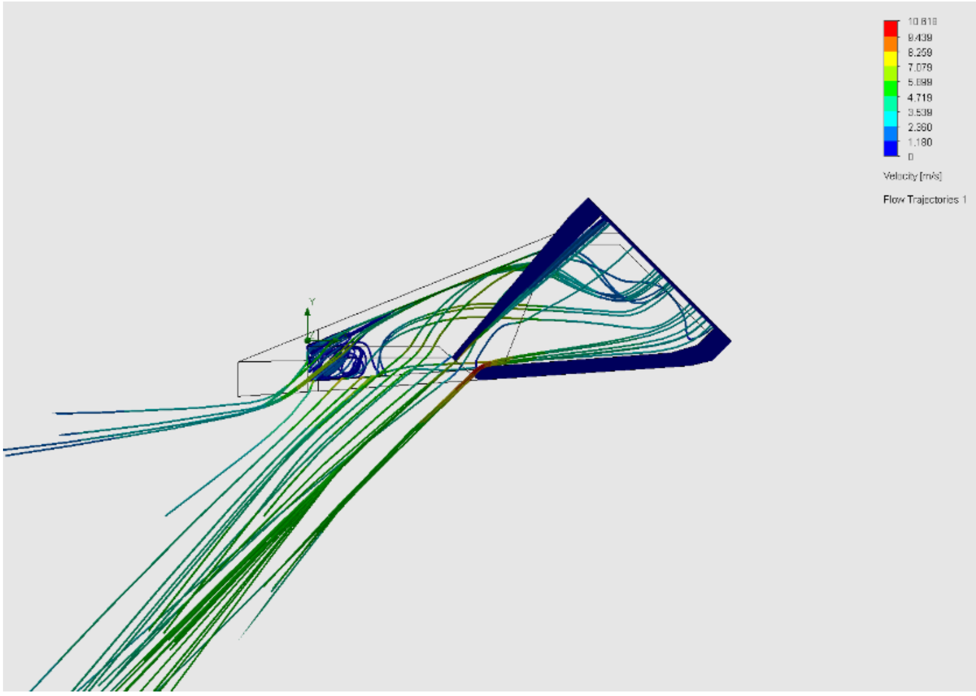

Figure 2.13 A simulation showing the CFDM fan shroud being able to direct air downwards in an approximate 45° angle to cool effectively.

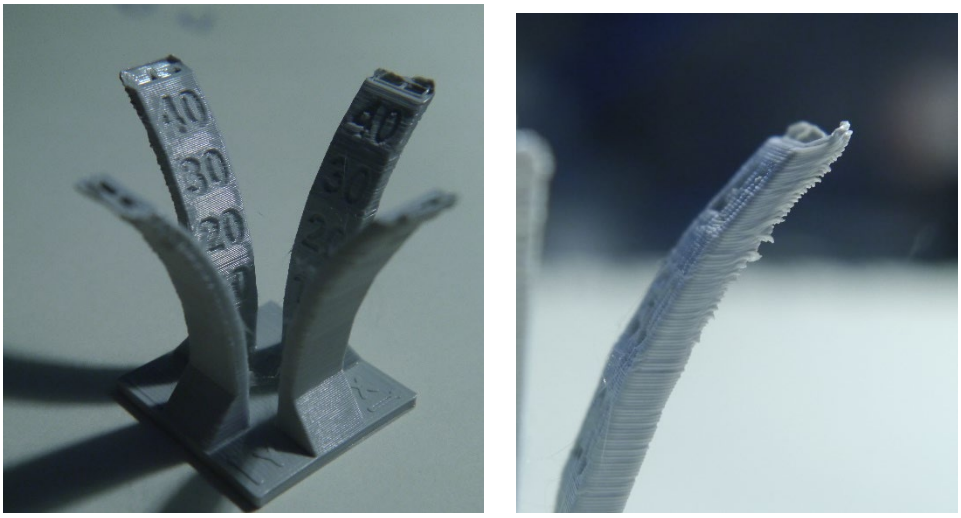

Figure 2.12 Overhang test without fan in PLA. Left: The numbers indicate where the print failed, which was on the transition to 45°. Right: Curling of the test with no fan due to laying down filament on still hot material.

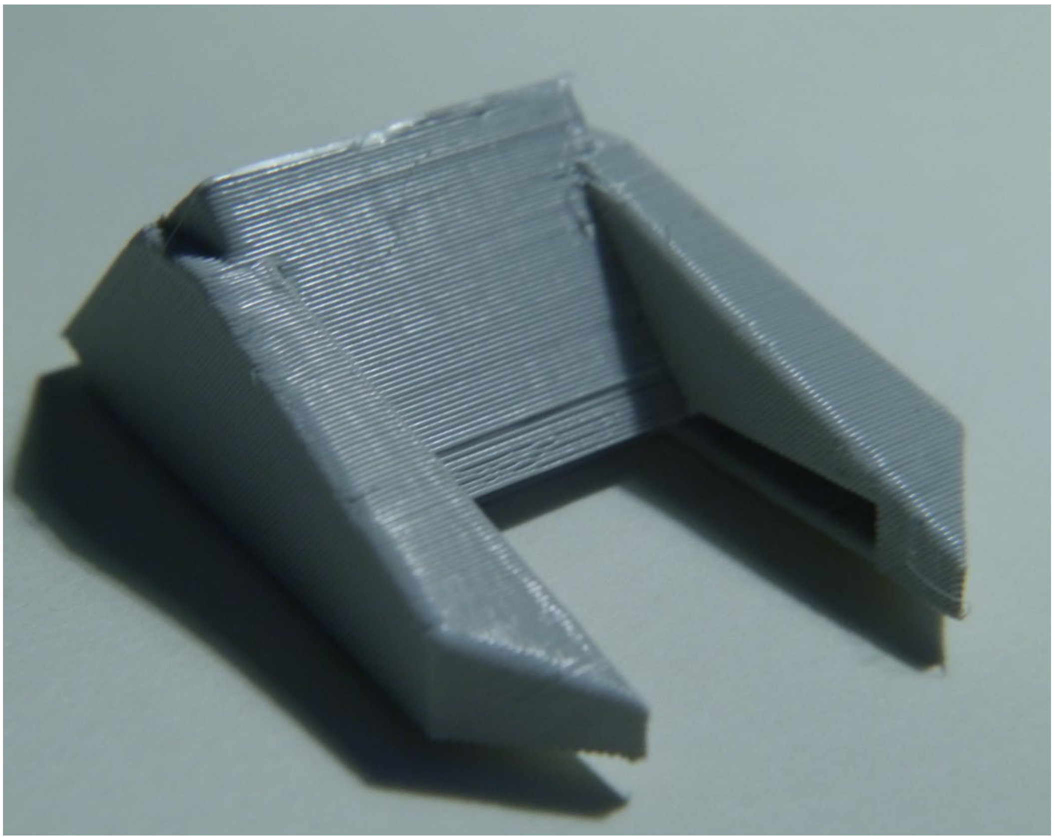

Figure 2.14 The finished fan shroud printed in PETG.

2.4.3 **Height adjustment for bed level sensor**

For the leveling of the bed in preparation of a print there exists a sensor that measures a grid of points on the printer bed. This ensures that the bed is level and adjusts the printer to account for small differences in height between points. The sensor is held approximately 1-2mm above the nozzle tip to achieve its function.

A height adjustment mechanism for the sensor was created to enable its position to be raised and lowered to allow for bed levelling before a print and collision free movement of the extruder during printing, see Figure 2.15. The final design was made with a locking ring to allow the sensor to be lowered to its original position for repeatable results during printing. A more detailed view of the height adjustment assembly can be seen in appendix B.4.

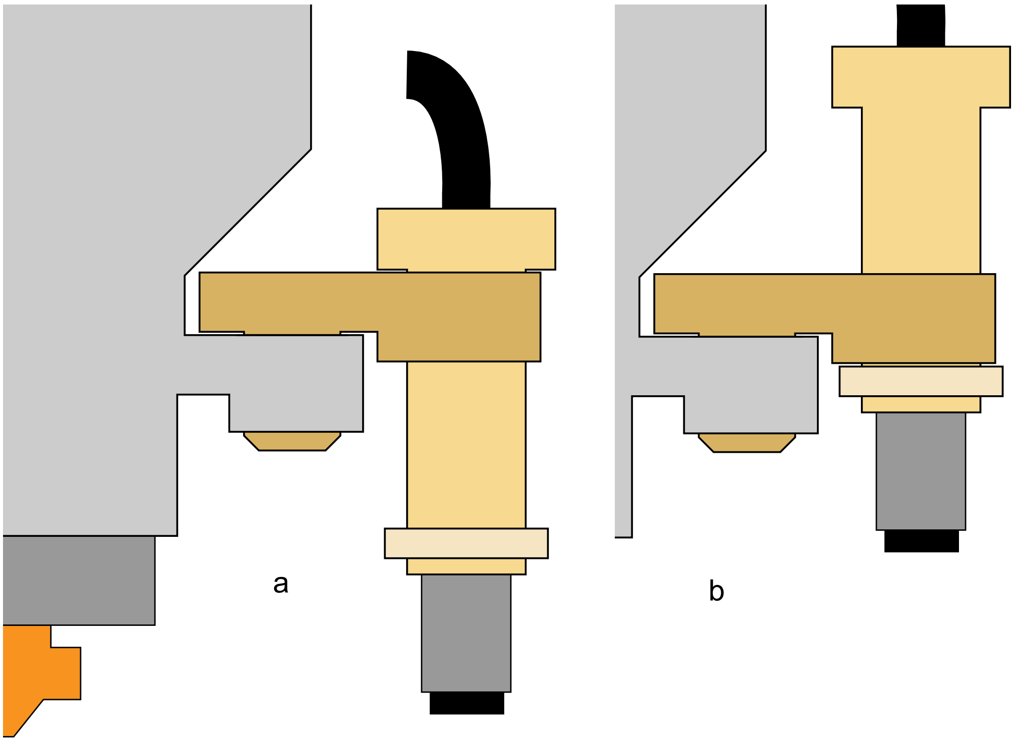

Figure 2.15 The lowered (a) and raised (b) positions of the height adjustment mechanism.

3 Methods

3.1 Hardware

The 3-axis printer Prusa MK3s+ was used to apply the hardware modifications to and test the non-planar operation of. The adjustments proposed and implemented from chapter 2 can be summarized and seen in Figure 3.1. The modified extruder is capable of non-planar printing with larger surface angles and in a larger area.

The work uses pre-existing software for non-planar printing as described in chapter 2.3.2, where a presented 3d model is sliced conventionally but capped with non-planar layers. The hardware of the printer is modified for greater clearance and non-planar printing capability for use with the software. The extent of changes necessary came from the literature review, as well as the test printers construction, which gave insight into what a reasonable level of clearance would be in terms of effort and time usage. The modifications made and the clearance around the nozzle can be seen in Figure 3.1.

3.2 Experiments

As a design of experiments approach would be used in the course of this project the determination of possible valuable process parameters necessitated some simpler test series. These tests gave information about the more and less important factors and their limits when printing so as to not cause print failures during the DOE.

The measurement of surface quality for non-planar parts will be done through analysis of images of the test prints. An area measurement of the surface defects will be taken and compared to the nominal area of the test part to calculate a percentage fault level as a measurement to compare parts.

Statistical analysis of the measurement runs will be done to establish if the results are significant and to what degree each factor has an impact.

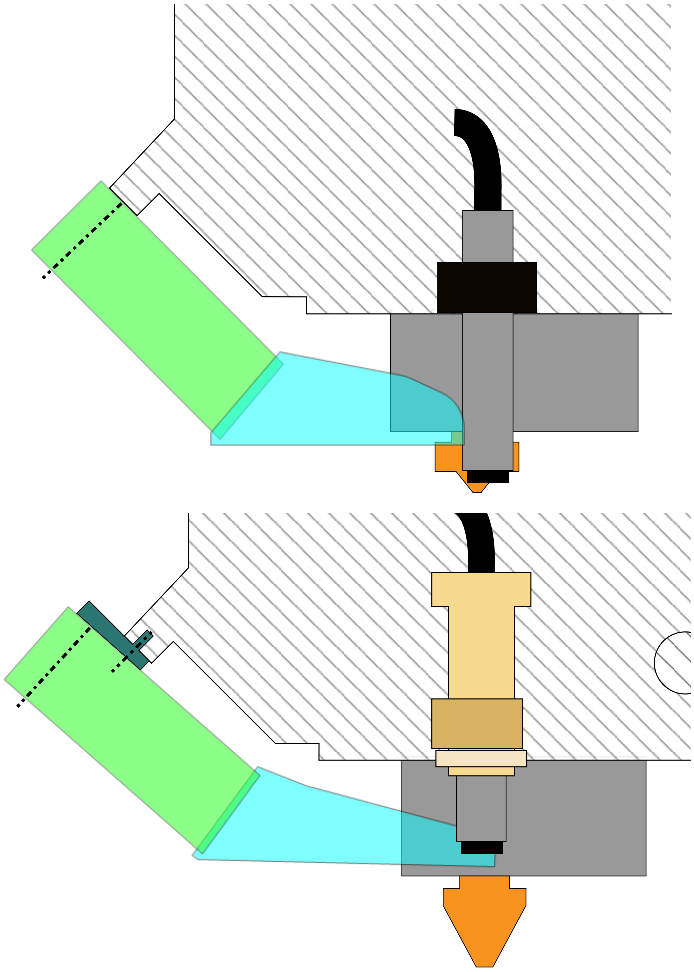

Figure 3.1 The changes made to the extruder with the old configuration above and the new configuration with fan shroud, height adjustable bed level probe and nozzle.

4 Preparation for experiments

4.1 Goal function of the experiment

To get a comparable result for the test models in the DOE experiment a model for surface defects was constructed. The approach used experience gathered from experience with the slicer software and its resulting parts to identify areas of the parts which suffered from defects. The 4 major categories of surface faults were found to be:

- Ridging - The accumulation of material between filament paths when printing at more acute angles (Figure 4.1B and D)
- Over extrusion – Accumulation of plastic in certain areas due to either nozzle interference (dragging the plastic along) with previously extruded plastic or incorrect flow from the nozzle (see Figure 4.1A).
- Visible previous layers – A previously printed layer can be seen in the top surface. Visible as lines normal to the top printed surface extrusions (see Figure 4.1C).
- Surface trueness – The dividing lines between different areas of the print and how visible they are (see Figure 4.2).

For the goal function these different defects would then be summarized to acquire a percent value of total defect for each of the analysed samples. The goal of the tests would then be to find the parameters which showed the greatest effect in minimizing the total surface defect percentage. The model the tests were based upon was made to provide representation of the different printing issues which were deemed to be useful for testing and were formerly encountered when exploring factors to be used for the design of experiments analysis.

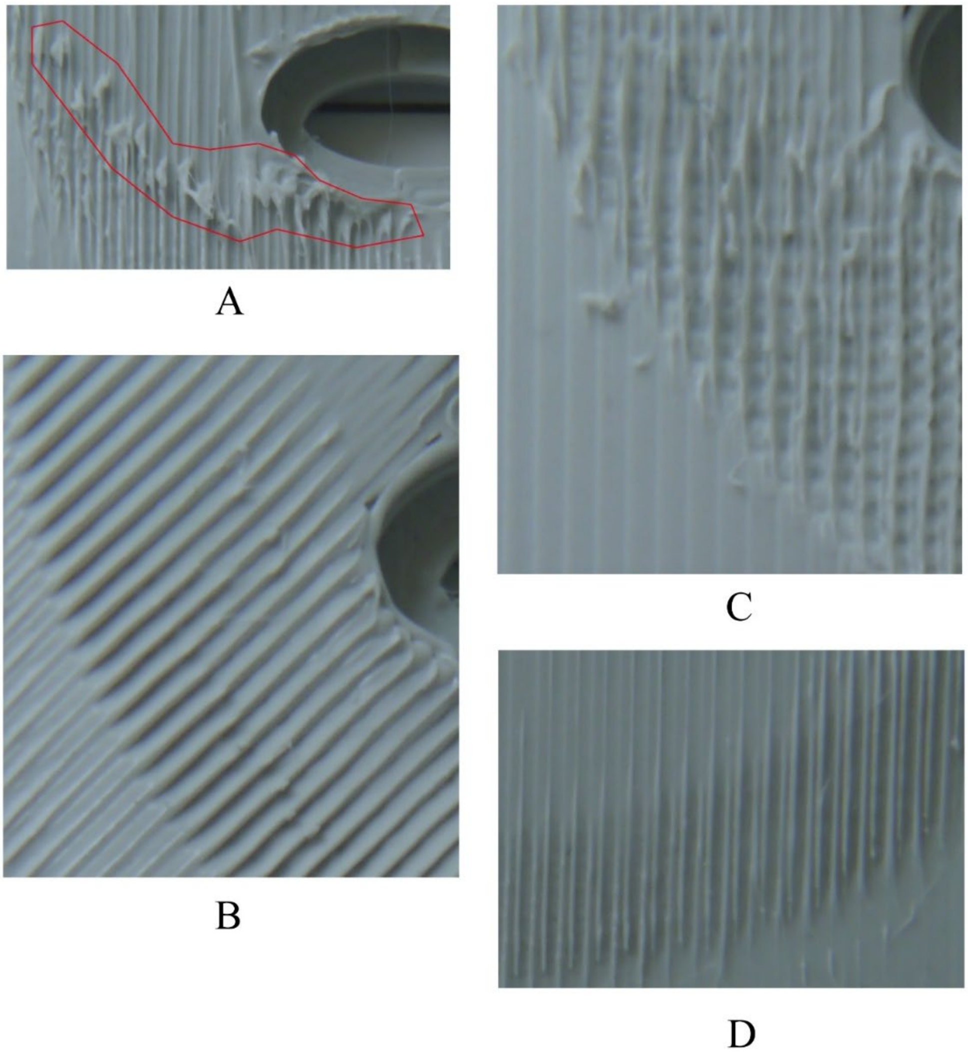

Figure 4.1 The diverse types of surface defects that were measured in the experiment. A – over extrusion, marked in red. B – Ridging, also seen in D. C – a previous layer can be seen through the top surface visible here as horizontal lines.

Figure 4.2 The picture shows what areas of the part has defined lines between the different surfaces of the model, marked in blue. This was compared to the 3d-models values for the perimeter length projected to a 2d.

4.2 Capture Setup for Samples

The processing of the samples necessitated a standardized approach in the capturing of the photos for analysis as to minimize deviation in area and perimeter length as these factors would impact the result when comparing with the values originating from the 3D model.

A picture captured with a fixed mounted light source as well as a sample holder to ensure repeatable placement of the samples in a photo box, see Figure 4.5. A camera (Panasonic DMC-GX1) was then placed at a fixed distance from the sample in another fixture (more clearly visible in appendix B.5) to the be able to capture a photo with the test subject laid out on a grid with known dimensions, see Figure 4.3. The grid aimed to ease the use of lens correction[1] tools in the image manipulation software Photoshop 2023 as well as sample alignment. The same process was to be applied on all sample photos to ensure proper placement and low distortion for the following step.

The measurement of the surface fault was then completed in Adobe Illustrator V27.11 where areas of surface defects were observed and noted as a percentage fault of the total area and perimeter, which served as the goal parameter to minimize Figure 4.4. The built-in perimeter measurement tool was used to measure surface trueness and a plugin for calculation of area in Adobe illustrator (Buchanan, 2018).

[1] A camera lens will distort a photograph but there exists methods for removing this.

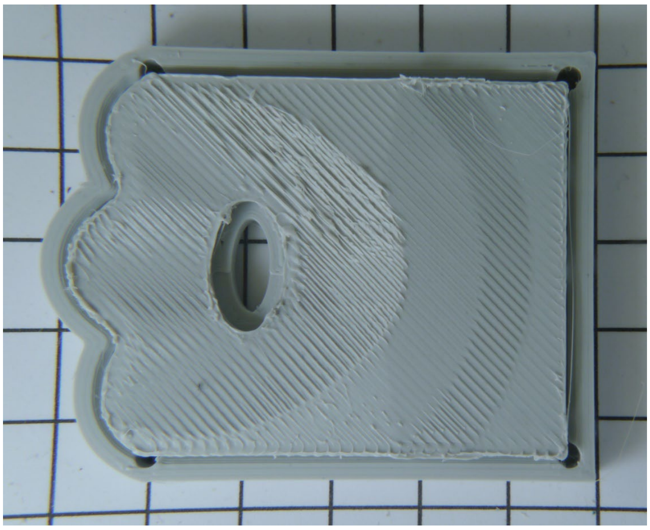

Figure 4.4 A sample picture after correction of lens distortion with the alignment grid in the background.

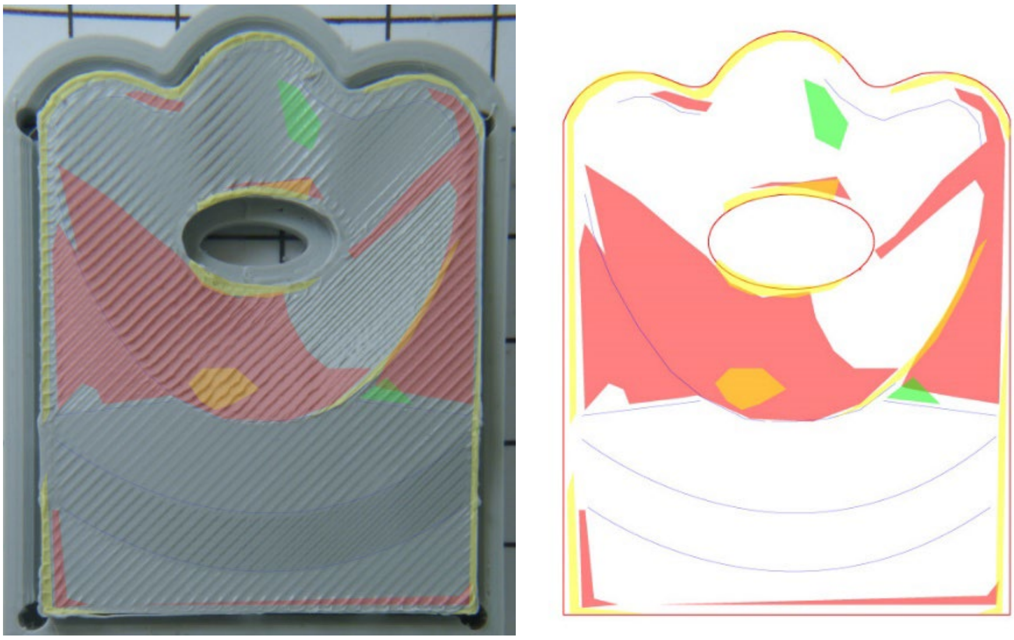

Figure 4.3 Left: A sample from the test process which has all fault areas marked. Right: The same fault areas compared to the 3d test models perimeter outline in red.

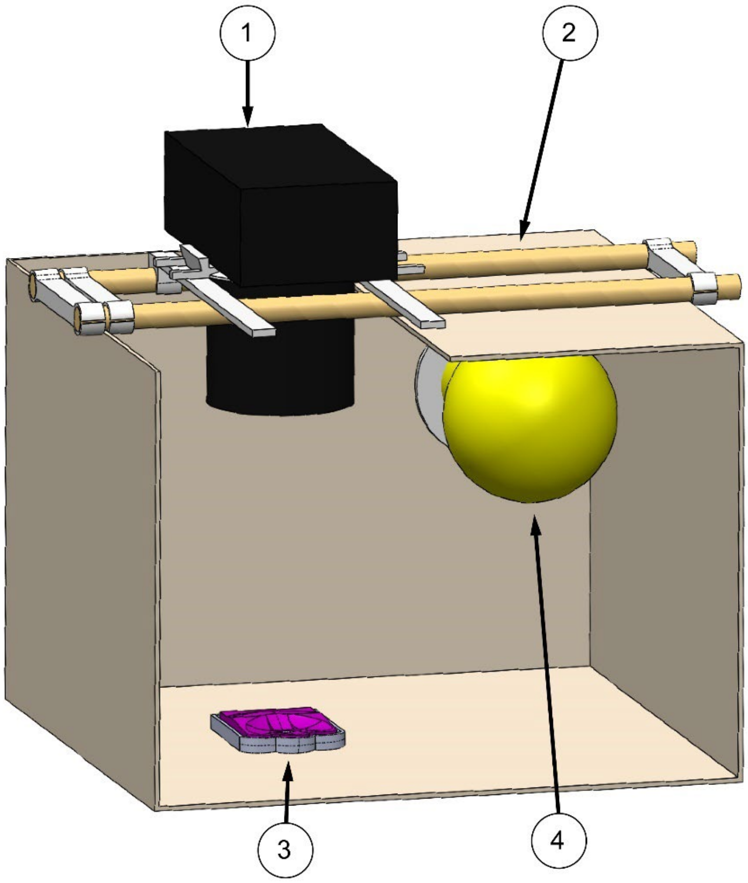

Figure 4.5 The setup for capturing sample photos. 1 - Camera. 2 - Fixture to hold camera to capture box. 3 - Sample holder with sample in purple. 4 - Light source.

4.3 Design of experiments

4.3.1 **Experimental design**

The methodology of Design of Experiments (DOE) is used to expand user knowledge of different effects of parameters the given process. This is achieved through designing an experiment which measures the results from the experiment through the lens of specific parameters concurrently and the interactions between these.

Then be able to research the individual interaction between parameters in an effort to better understand the machine, the process, and the result. The effort results in a more clearly defined process where a better end result can be achieved through the knowledge of the individual parameters. DOE requires some experience of the process being analysed before the experiment is designed to determine the process parameters to be tested from all possible ones.

As the technology of CFDM and the specific software used is a relatively new area of study, the Design of Experiments factors were first derived from smaller 2 factor factorials tests prints where the effect of two different printing parameters were tested. The approach mixed increasingly complex and challenging models in terms of surface complexity and angle to the nozzle to extract the high and low values for the process parameters by reaching print failure then backing off slightly from the value at failure.

4.3.2 **Process variables**

To choose the process variables both experience gained from conducting practical tests and other works informed the decisions. The summarized process variables with identification letters and low-high level values are collected in Table 4.1.

- A- tip angle: A theory from (Ahlers, 2018, ss. 34-36) described the optimal nozzle for 3-axis CFDM as one where the flat surface diameter of the tip was made as close to the orifice diameter as possible. This variable is named the tip angle due to the addition of a secondary angle at the tip, which results in a flat tip area diameter of 0,6mm compared to the other nozzles 1mm diameter.
- B- Layer height: Due to the interference of the nozzle with the extruded filament while ascending or descending curves the layer height was seen as a reasonable parameter to include. It has in other works been seen to affect surface finish in planar printing (Ali, Chowdary, & Maharaj, 2014). The high and low values were chosen inside of limits often recommended

for 0.4 mm nozzles of between 25% to 75% of nozzle orifice diameter (Dwamena, u.d.).

- C- Movement acceleration of perimeters and infill: A parameter focused on exploring what impact the increased speed of high angle descents and ascents had.
- D- Solid infill fill angle: The angle of the infill that the top non-planar layers are oriented in. The influence of this parameter depends on model geometry due to some directions having more or less steep inclines generally.
- E- Nozzle temperature: Associated with strength and appearance of an FDM part. The inclusion of this factor was necessary to analyze its effect on non-planar surfaces. The values were chosen from filament manufacturer recommendations of high and low values.

Table 4.1 The five chosen process variables and their respective values for low (1) and high (2).

Process variable	A -Tip angle (°)	B- Layer height(mm)	C- Acceleration (mm/s²)	D- Fill angle (°)	E- Temperature(°C)
Low Value - 1	0	0,1	400	0	190
High Value – 2	30	0,3	2000	45	220

4.3.3 **Full factorial analysis**

A Full factorial analysis was used to analyze the process and determine the characteristics of it. A full factorial uses all possible variations of the process variable levels. The five chosen 5 process variables for the experiment varied over their 2 levels results in a total run of 2^5 or 32 samples to produce. A full factorial approach is useful if there is a need to further explore the main factor effects as well as the interaction between these factors and enables a structured approach to do so (National Institute of Standards and Technology, u.d.). In the case of this thesis the newness to the technology CFDM printing made a Full factorial analyses suitable to fully explore interactions and impacts.

For the planning of the run sequence of samples different random run orders were used for the sample printing and the two measurement runs to minimize the impact of uncontrollable factors on the experiment. The table for the design of experiment runs can be seen in Table 4.2 where interactions are also mapped. In Table 4.3 the run order of measurements taken can be seen. It also includes the recorded values for each run.

Table 4.2 The run mapping for the test sample creation. The table also shows interactions in the form of axb etc. in the blue columns.

	Sample number	A - Tip Angle [°]	B - Layer height [mm/s]	axb	C - Perimeter and top infill acceleration [mm/s2]	axc	bxc	dxe	D - Top surface fill angle[°]	axd	bxd	cxe	cxd	bxe	axe	E - Nozzle temperature[°C]
16	1	1	1	1	1	1	1	1	1	1	1	1	1	1	1	1
6	2	1	1	1	1	1	1	2	1	1	1	2	1	2	2	2
10	3	1	1	1	1	1	1	2	2	2	2	1	2	1	1	1
13	4	1	1	1	1	1	1	1	2	2	2	2	2	2	2	2
4	5	1	1	1	2	2	2	1	1	1	1	2	2	1	1	1
11	6	1	1	1	2	2	2	2	1	1	1	1	2	2	2	2
5	7	1	1	1	2	2	2	2	2	2	2	2	1	1	1	1
12	8	1	1	1	2	2	2	1	2	2	2	1	1	2	2	2
1	9	1	2	2	1	1	2	1	1	1	2	1	1	2	1	1
7	10	1	2	2	1	1	2	2	1	1	2	2	1	1	2	2
15	11	1	2	2	1	1	2	2	2	2	1	1	2	2	1	1
3	12	1	2	2	1	1	2	1	2	2	1	2	2	1	2	2
9	13	1	2	2	2	2	1	1	1	1	2	2	2	2	1	1
14	14	1	2	2	2	2	1	2	1	1	2	1	2	1	2	2
2	15	1	2	2	2	2	1	2	2	2	1	2	1	2	1	1
8	16	1	2	2	2	2	1	1	2	2	1	1	1	1	2	2
13	17	2	1	2	1	2	1	1	1	2	1	1	1	1	2	1
11	18	2	1	2	1	2	1	2	1	2	1	2	1	2	1	2
15	19	2	1	2	1	2	1	2	2	1	2	1	2	1	2	1
9	20	2	1	2	1	2	1	1	2	1	2	2	2	2	1	2
16	21	2	1	2	2	1	2	1	1	2	1	2	2	1	2	1
3	22	2	1	2	2	1	2	2	1	2	1	1	2	2	1	2
1	23	2	1	2	2	1	2	2	2	1	2	2	1	1	2	1
7	24	2	1	2	2	1	2	1	2	1	2	1	1	2	1	2
2	25	2	2	1	1	2	2	1	1	2	2	1	1	2	2	1
5	26	2	2	1	1	2	2	2	1	2	2	2	1	1	1	2
8	27	2	2	1	1	2	2	2	2	1	1	1	2	2	2	1
14	28	2	2	1	1	2	2	1	2	1	1	2	2	1	1	2
4	29	2	2	1	2	1	1	1	1	2	2	2	2	2	2	1
10	30	2	2	1	2	1	1	2	1	2	2	1	2	1	1	2
12	31	2	2	1	2	1	1	2	2	1	1	2	1	2	2	1
6	32	2	2	1	2	1	1	1	2	1	1	1	1	1	1	2

Table 4.3 The measurements taken during the DOE. Both runs have a separate randomized order of testing.

Randomized order	Sample number	Run 1 - Total fault [%]	Randomized order	Sample number	Run 2 - Total fault [%]
17	1	74,62%	3	1	67,74%
31	2	65,68%	19	2	60,88%
19	3	59,09%	15	3	68,33%
26	4	63,21%	28	4	65,21%
22	5	48,02%	10	5	53,83%
14	6	61,43%	17	6	49,15%
28	7	59,32%	11	7	66,29%
9	8	69,49%	24	8	69,93%
4	9	53,18%	30	9	60,99%
8	10	39,43%	8	10	47,76%
3	11	62,89%	32	11	72,60%
1	12	67,40%	16	12	70,19%
16	13	62,93%	18	13	64,86%
6	14	39,92%	22	14	42,07%
13	15	73,41%	14	15	77,11%
7	16	57,71%	23	16	64,03%
10	17	48,39%	13	17	52,57%
11	18	27,62%	26	18	31,43%
15	19	58,59%	6	19	53,02%
32	20	48,20%	25	20	59,54%
21	21	25,97%	9	21	30,51%
30	22	15,26%	7	22	22,29%
27	23	41,05%	1	23	48,88%
20	24	41,73%	27	24	46,09%
5	25	22,44%	5	25	34,66%
18	26	34,19%	12	26	37,36%
2	27	59,92%	21	27	62,36%
25	28	40,22%	4	28	52,71%
29	29	38,46%	31	29	40,23%
24	30	32,25%	20	30	38,52%
23	31	64,13%	2	31	67,10%
12	32	51,42%	29	32	62,06%

4.4 Test part

The design of the test part was an attempt to capture a part which encompassed as many areas as possible where surface defects were detected in other parts. Figure 4.6 shows the final test part used. The feature were chosen to be an acceptable representation of many aspects of non-planar printing, while also printing fast with simple print preparation between samples.

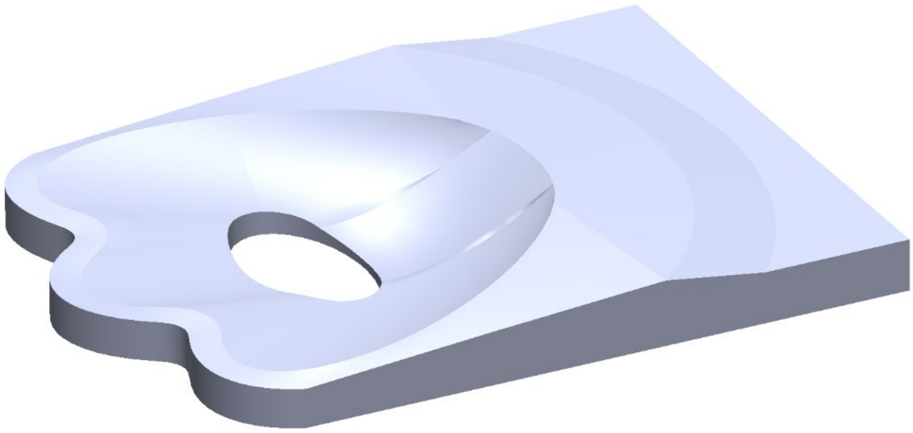

Figure 4.6 The test part used for design of experiments. Intended to test various problem areas that had been found while printing non-planar parts.

Figure 4.7 shows the 3d model of the test part divided into the general areas being showcased. There will now be an effort to describe its different parts:

a. A thin strip around the scalloped area b, these areas are prone to over extrusion and the large perimeter was meant to prove a tough obstacle in terms of showing a clear dividing line between surfaces.
b. A scalloped area with a surface angle of approximately 35° with the border to area c rounding out to a flat and then ending with a sharp edge towards area a. The effects of ridging and over extrusion are very apparent in curved areas and depending on the parameters when printing spread somewhat to surrounding areas.
c. A shallow angle (~5°) flat area which is included to test the high angle transition from the nozzle approaching from surrounding areas.
d. An area with slight curvature in both directions with a moderate surface angle(~10%) captures if dragging of the plastic filament by the nozzle occurs at some parameter even at relatively low angles.

e. A flat area to benchmark the sample parts performance in also doing planar geometry when included in a part also consisting of non-planar areas.

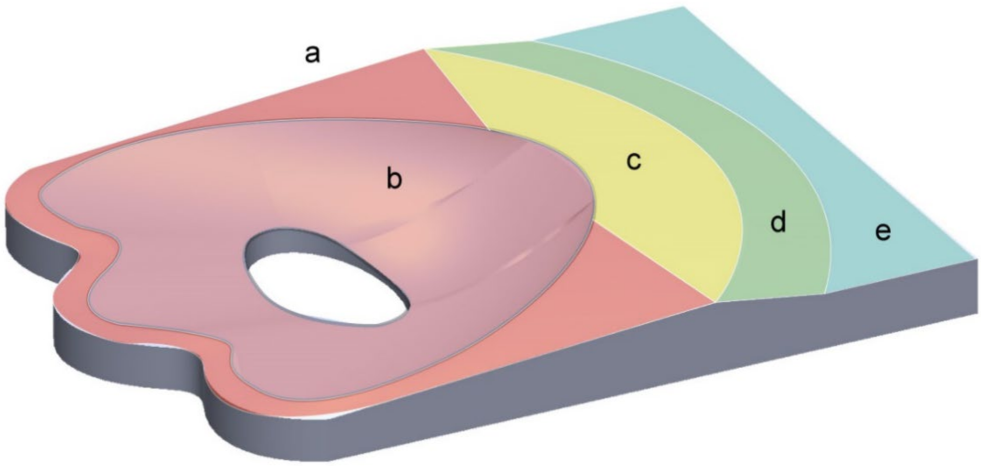

Figure 4.7 The test part divided in areas of importance.

5 Results

5.1 Analysis of measured values

5.1.1 **Significance of measured values - ANOVA**

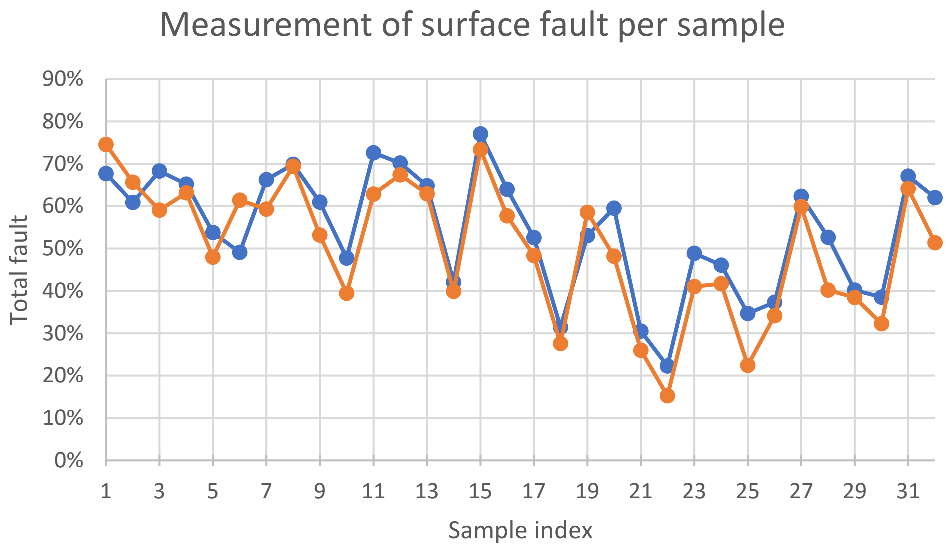

Figure 5.1 The total fault per sample over two different measurement runs for all samples.

Figure 5.1 shows the two series of measurements taken on the 32 samples for a total of 64 measurement points total. The relatively good fit between the two measurement runs indicates that the measurement method was not varying greatly over separate runs and when done in random order to each other. To evaluate the significance of measurement technique used, an Analysis of Variance (ANOVA) was done across the two measurement populations. The results, see Table 5.1, can be summarized as follows:

- The P-value of 5,45E-13 can be compared to the chosen α-value of 0,05. As the P-value is much lower than the α-value the affirmation of a highly significant difference between sample values across the runs can be made.
- The individual sample measurements are however shown to have a significant correlation. Indicating that the measurements were repeatable, and the sample-to-sample mean differences were much greater than that from separate measurements on the same sample. This can be seen by the calculated F-value being much smaller than the F-critical.

$$F = 18{,}01355 \gg F_{crit} = 1{,}810379 \tag{5.1}$$

- The null hypothesis of no difference between sample means can be rejected due to both the low probability value and F being much larger than F critical as seen in eq.(**5.1**).
- An alternate hypothesis of the existence of a significant difference between sample surface faults can be assumed.

Table 5.1 ANOVA analysis results

ANOVA

Source of Variation	SS	df	MS	F	P-value	F crit
Between Groups	1,321941	31	0,042643	18,01355	5,45E-13	1,810379
Within Groups	0,075753	32	0,002367			
Total	1,397694	63				

5.1.2 **Measurement of different result parameters**

When dividing the total fault into its component parts of over extrusion, perimeter trueness, ridging and previous layer visibility the results seen in Figure 5.2. Showing that generally the perimeter trueness was the greatest portion of the fault for most samples with ridging being the second largest fault.

- It is interesting to note that in some samples faults related to over extrusion (such as sample 18-19) and visibility of previous layers (sample 4 and 8) could be almost completely eliminated.

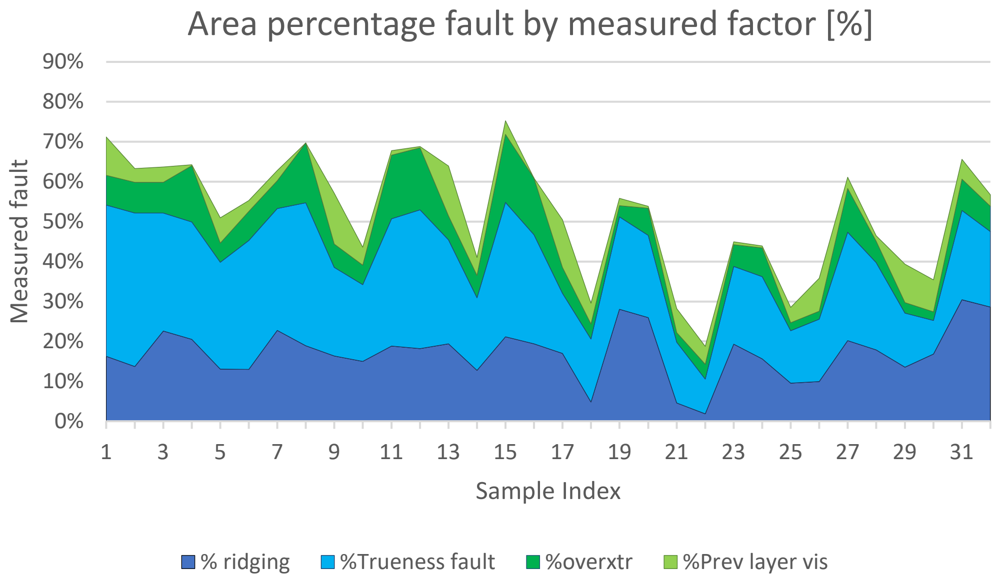

Figure 5.2 Stacked area graph of the different measured area defects.

5.2 Analysis of factors and interactions

5.2.1 **Main factor effects**

To understand the impact of each main factor they are separated through looking at the averages of each sample with the factor low and factor high value of factor. Figure 5.3 visualizes this and shows:

- The tip angle of the nozzle (A) was the most dominant factor. With a -17% change between low and high mean values. Indicating that it is an important factor in this process.
- The second most significant main factor was the surface fill angle (D). With a +15% difference between mean low and high.
- The third most significant factor was the temperature (E) with a -6% change between mean low and high. Further analysis needed to show if it is significant.
- Both the layer height (B) and acceleration (C) showed little importance for the total surface fault in this analysis and might have low impact on the process.

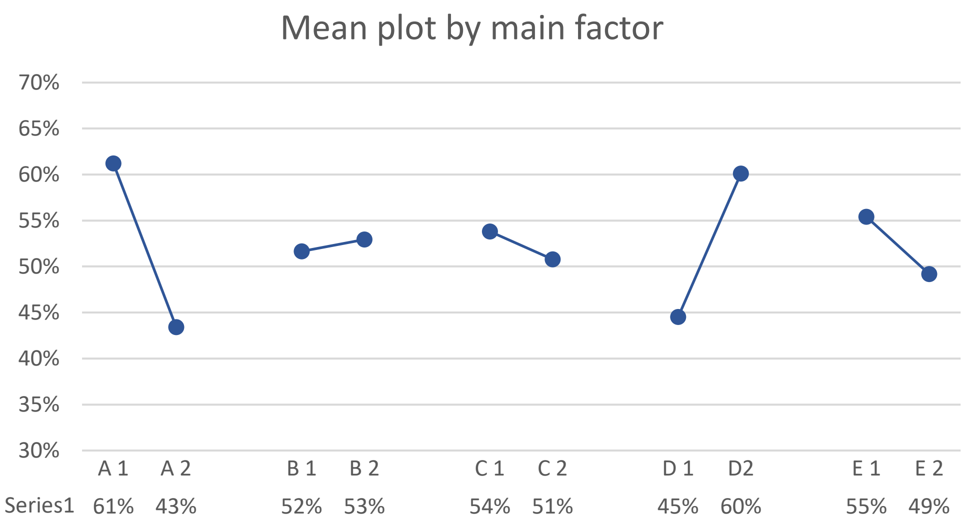

Figure 5.3 The main factor mean effects on the total surface fault [%] of the test parts. The graph shows that the Nozzle tip angle (A), surface fill angle (D) and temperature(E) had the largest effect on the surface fault in descending order.

5.2.2 Significance of main factors

A box plot was made to see how the main factors high and low value varies amongst their population. The insight gathered from Figure 5.4 is as follows:

- Factor B and C (layer height and acceleration) show large overlaps of low- and high-level bodies[2] (B1-B2 and C1-C2) in the box plot with a spread of (52,4%;46,71%) and (42,63%;56,48) respectively. This strengthens the argument that these main factors are not significant on their own.
- The nozzle angle low-high box plot shows the least body overlap as well as the highest position mean of 61,21% when the factor is low. This further indicates the significance of this factor combined with the relatively low variance compared to the other main factor box plots.
- The solid infill angle (D1-D2) shows a similar but smaller difference in body position with some overlap as well as a large variance in total fault values.
- For the temperature E1-E2 there is a slight downward trend of surface fault when it is set high. Although the overlap means that no strong conclusion can be drawn yet.

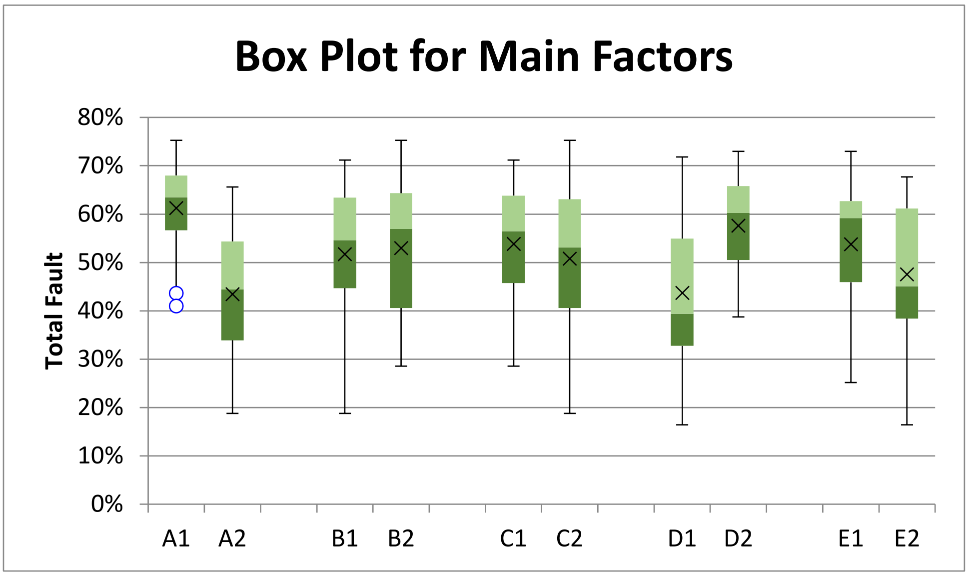

Figure 5.4 To further investigate the significance of main factor a box plot was made. The individual plots show the mean value as an x. The upper and lower quartiles in green. Maximum and minimum bounds indicate maximum and minimum values for each group, except outliers marked with a blue circle.

[2] The middle 50 percent of values.

5.3 Interaction means

5.3.1 **Pairwise parameter interactions**

Figure 5.5 shows a table of all interaction graphs where all the possible pairwise interactions between main factors have been included. The largest interactions between the most influential parameters were further studied by deconstructing the interactions by separating each interaction graph into two lines, where the levels are varied. By doing this further information can collected on the nature of the interaction.

Looking again at Figure 5.5 the influential interactions AxB, AxD, AxE and BxC were chosen due to either being an interaction that showed a big change in the goal function or the strong interaction of a previously established influential main factor (A) with other parameters.

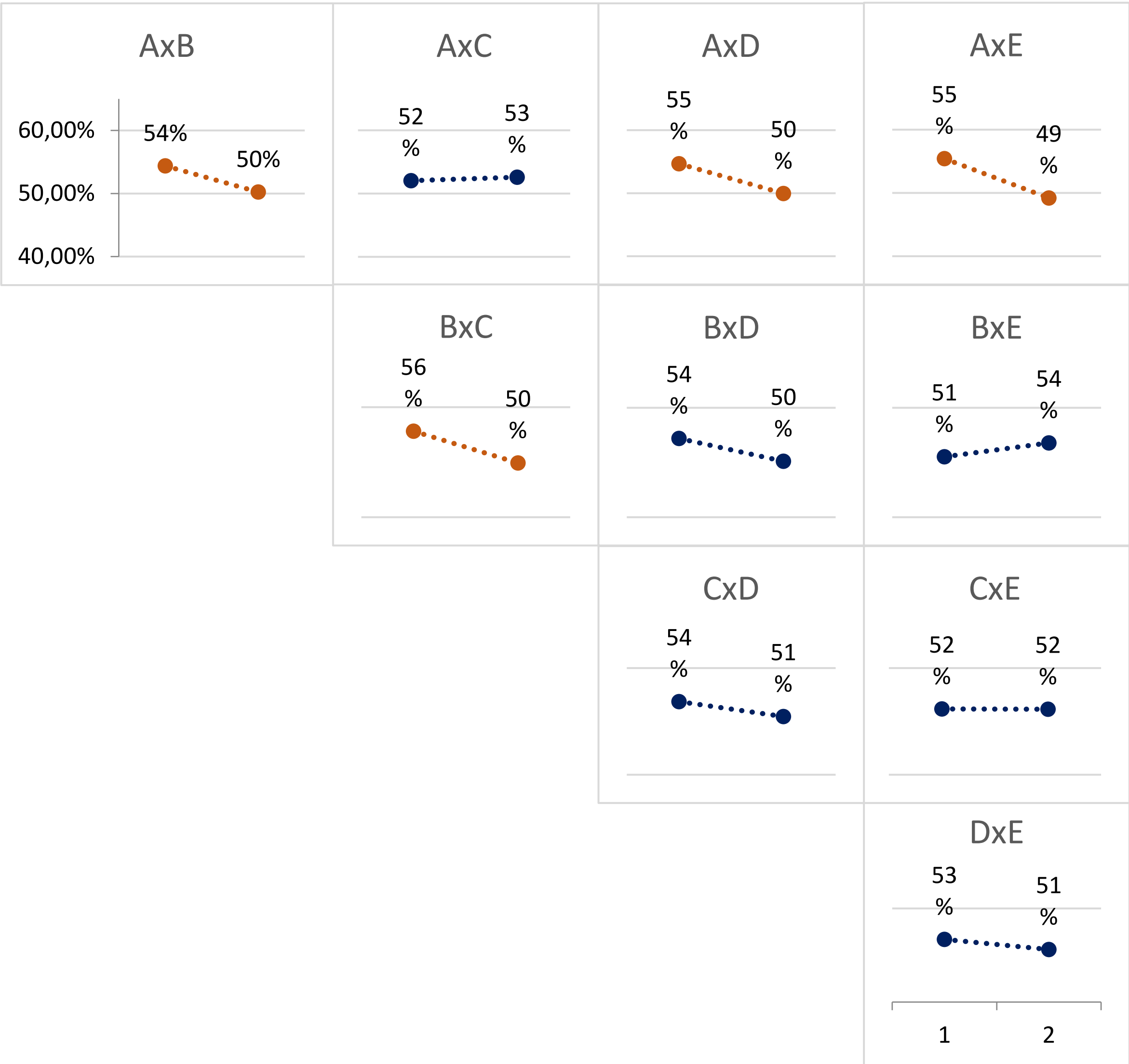

Figure 5.5 The plots for all main factor interactions. The 4 largest interactions (AxB, AxD, AxE and BxC) have been marked in orange and will be further analyzed by further separating the interaction means into component parts. A – Nozzle tip angle, B – Layer height, C – Acceleration, D - Fill angle, and E – Temperature.

5.3.2 **Measuring cross effect, divergence, and convergence**

The results in Figure 5.6 give the following information of the interactions:

- Nozzle tip angle and layer height experience a cross effect where the layer height only makes a small difference for the goal function with the low angle nozzle but for the 30° tip nozzle shows some indication of lowering the surface fault with lower layer heights. The difference in mean surface fault between A2B2 and A2B1 is however not that large (5,4%) and might not be significant.
- Nozzle angle and temperature show little to no interaction in their effects as the two lines are almost parallel.
- Nozzle tip angle and top surface fill angle show some divergence where the effect of the surface fill angle increases with the 30° tip nozzle. This can perhaps be partly explained by the nozzle angle being less prone to dragging material with it and the main effect of the showing less overall surface faults with the surface fill angles low value (0°).
- Layer height and acceleration shows acceleration having a low impact when the layer height is high (B2) and playing a larger part when the layer height is low(B1). The large spread of the measured values which was previously seen in Figure 5.4 for B and C do not allow for evaluating if this interaction is significant.

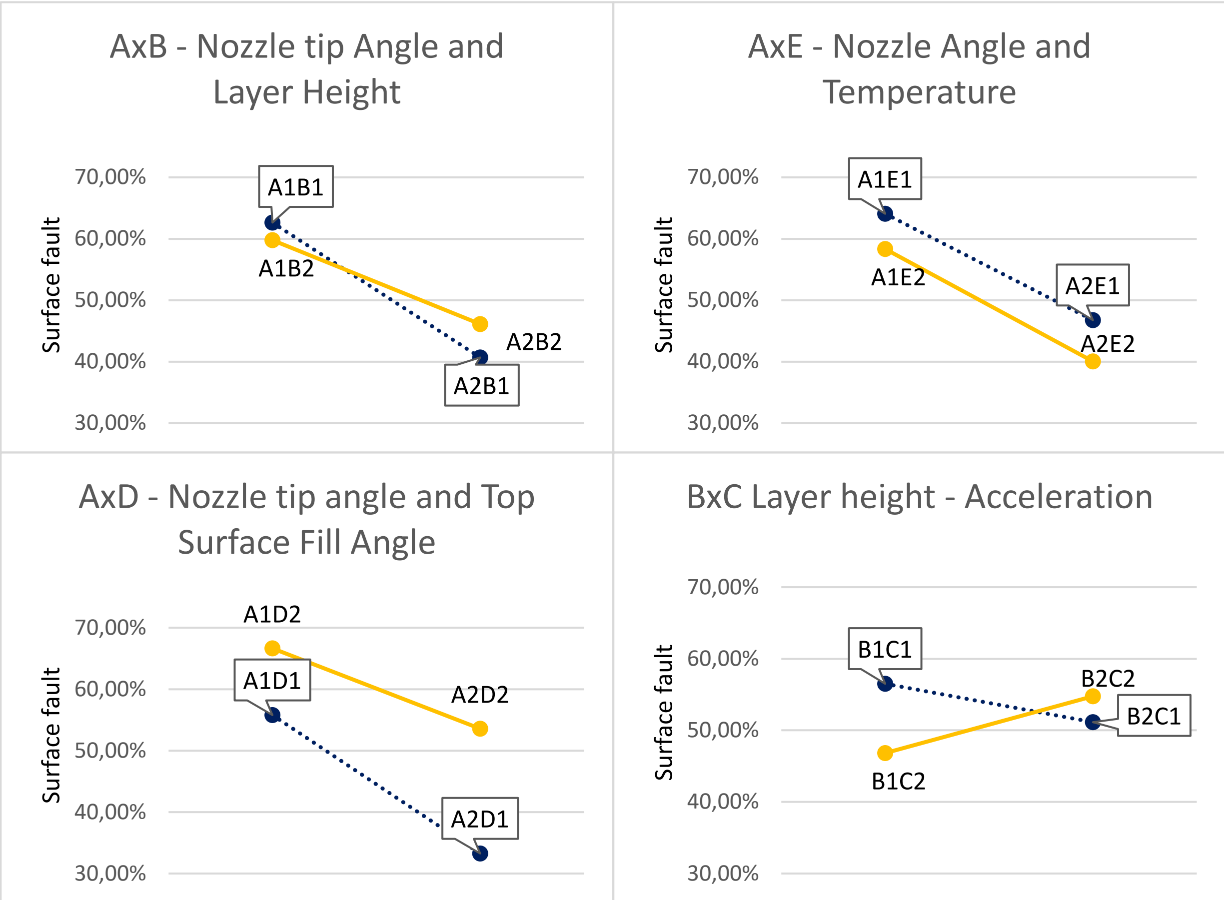

Figure 5.6 Visualization of the high impact interactions from Figure 5.5 by showing how one parameter impact changes based on another.

5.4 Conclusion of design of experiments results.

- The dominant main factor was the shape of the nozzle tip which showed the largest impact on surface defects at a tip angle of 30°. It was also shown to be the most significant factor among all main parameters and interactions.
- The surface fill angle was the second most dominant when set at 0°. This parameter relates more to an individual models geometry but shows what impact changing this parameter can have on surface defects in a non-planar print.
- The interaction between fill angle and nozzle tip showed a positive interaction with the 30° tip and a fill angle of 0°.
- The temperature of nozzle showed some impact during the tests but would need further tests to establish the extent of the impact. The high value of the nozzle temperature at 220°C carried the fourth greatest improvement surface defect minimization.

The conclusion to be drawn from this is that for the purpose of 3-axis CFDM the nozzle design is of great importance, as well as orienting the travel paths to enable the nozzle to travel over areas at the shallowest angles when possible.

While the measurement model worked to identify some significant factors, the variance made it unsuitable for evaluating lower impact results significance.

6 Discussion

6.1 Reflection

The goal of the thesis was to modify a 3-axis consumer 3d printer for the purpose of enabling use of CFDM technology and evaluating the performance of the technology and measurement method in turn by design of experiments. An insight after the fact was that the modification of hardware posed a problem to the time plan, as the testing of CFDM parameters and other hardware prototypes depended on the machine already being capable of a higher level of non-planar printing. The approach of using previous work combined with experience from planar FDM to devise a reasonable design space for the nozzle design made the prototyping of it possible in only a few iterations. This approach was a valuable insight into building and synthesising data from others in the form of reports, forums, or blogs into productive results.

A reflection on the process was that the choice of a full fractional design should have been considered more thoroughly. The choice was made with the intention to gather enough data for a better evaluation of the measurement system used over a large number of groups, as well as to explore all interactions between parameters fully. But in retrospect this would have probably been better served if more measurements were done over a smaller population with a fractional factorial design to more easily prove or disprove significance among the gathered results. In opposition to this a fractional factorial may not reveal as much in regard to interactions between parameters.

The width of the parameter values used for the DOE were made as large as possible. Using the extreme values of each parameter aimed to capture impacts at the edges of what the process is capable of but neglects middle values which, if used, could show a non-linear impact of a given parameter. Tests using values at more than 2 levels would be useful to explore this but take more time and require more samples, due to time limitations this was not done.

6.2 Future work

In the future a continued investigation of the role of the nozzle geometry should be done, as it stood as the single most important factor from testing. The design was also kept quite conservative with an angle of only 30° from horizontal, therefore a series of tests varying the nozzle angle across more levels would serve to map the relation of nozzle angle more clearly to surface quality.

The design of experiments showed some interesting results but might reveal more if for example a 3-level analysis were to be done for some of the process parameters. For example, the impact of the nozzle temperature might be greater in the middle between the values used in this report's study which would not be captured if not tested for. This could be accomplished in a larger study as the number of samples would increase, even if using a fractional factorial DOE.

A standard benchmark non-planar print for surface quality measurement would be useful to develop in the future. This would make the results more comparable between reports and probably lead to more accurate results.

If the measurement system for surface defects used in this report should be used in the future a way of expediting the process should be considered. For example, 3d scanning which could help in both lowering the influence of human error and allow for more accurate and fast measurements of the surface quality.

References

3DPotter. (2023, January 2). *3D Potterbot 10 Micro*. Retrieved from https://3dpotter.com/printers/potterbot-micro-10

3DSourced. (2021, August 10). *The Complete History of 3D Printing: From 1980 to 2022*. Retrieved September 25, 2022, from https://www.3dsourced.com/guides/history-of-3d-printing/

Aerovent. (2018). *Fan engineering - Surge, Stall, and Instabilities in Fans.* Retrieved December 13, 2022, from https://www.aerovent.com/wp-content/uploads/2018/12/Surge-Stall-and-Instabilities-in-Fans-FE-600.pdf

Ahlers, D. (2018). *3D Printing of Nonplanar Layers.* Hamburg: MIN-Fakult¨at.

Ali, F., Chowdary, B. V., & Maharaj, J. (2014). Influence of Some Process Parameters on Build Time , Material Consumption , and Surface Roughness of FDM Processed Parts : Inferences Based on the Taguchi Design of Experiments. *The 2014 IAJC/ISAM Joint International Conference.* Orlando.

Autonomous Manufacturing. (2023, January 3). *Industrial Applications of 3D Printing:*. Retrieved from AMFG: https://amfg.ai/industrial-applications-of-3d-printing-the-ultimate-guide/

Bigrep. (2021, July 12). *FDM Vs. SLA 3D Printer: Choose The Right Technology*. Retrieved November 24, 2022, from https://bigrep.com/posts/fdm-vs-sla-3d-printer/#:~:text=In%20general%20SLA%203d%20prints,SLA%20print%20will%20be%20smoother.

Buchanan, B. (2018, July 28). *Script to find the area of shapes in Adobe Illustrator*. ([bryanbuchanan], Producer) Retrieved November 25, 2022, from Github: https://gist.github.com/bryanbuchanan/11387501

Chakraborty, D., Reddy, B., & Choudhury, A. (2008, February). Extruder path generation for Curved Layer Fused Deposition Modeling. *Computer-Aided Design*, pp. 235-243.

Dwamena, M. (n.d.). *Which Layer Height is Best for 3D Printing?* Retrieved November 20, 2022, from 3dprinterly: https://3dprinterly.com/which-layer-height-is-best-for-3d-printing/

Filemon, S. (2016, May 16). *How expiring patents are ushering in the next generation of 3D printing*. Retrieved September 25, 2022, from Techcrunch: https://techcrunch.com/2016/05/15/how-expiring-patents-are-ushering-in-the-next-generation-of-3d-printing/?guccounter=1&guce_referrer=aHR0cHM6Ly93d3cuZ29vZ2xlLmNvbS8&guce_referrer_sig=AQAAANgMOe8ETHYoEaZLGXfuCCTA6yJd8vFvi3RsUWVRVbBKhI2efH0QGM0JSLlCNc9k8HZ

Formlabs. (n.d.). *Guide to Stereolithography (SLA) 3D Printing*. Retrieved December 12, 2022, from https://formlabs.com/eu/blog/ultimate-guide-to-stereolithography-sla-3d-printing/

Formlabs. (n.d.). *SLA compared to FDM.* Retrieved December 30, 2022, from https://formlabs.com/blog/fdm-vs-sla-compare-types-of-3d-printers/

JoshuaRowley42. (2017, January 27). *V6-NOZZLE-ALL*. Retrieved October 15, 2022, from E3D-wiki: https://wiki.e3d-online.com/File:V6-NOZZLE-ALL.pdf

Lee, C.-Y., & Liu, C.-Y. (2019, January). The influence of forced-air cooling on a 3D printed PLA part manufactured by fused filament fabrication. *Additive Manufacturing, 25*, 196-203. doi:https://doi.org/10.1016/j.addma.2018.11.012

Mitropoulou, I., Bernhard, M., & Dillenburger, B. (2020). Print Paths Key-framing Design for non-planar layered robotic FDM printing. *Symposium on Computational Fabrication.* Virtual event. doi:10.1145/3424630.3425408

Mitropoulou, I., Bernhard, M., & Dillenburger, B. (2022). Nonplanar 3D Printing of Bifurcating Forms. *3D Printing and Additive Manufacturing, 9*(3), 189-202. doi:http://doi.org/10.1089/3dp.2021.0023

Mycusini. (n.d.). *mycusini® - Features & benefits*. Retrieved January 1, 2023, from https://mycusini.com/en/pages/mycusini

National Institute of Standards and Technology. (n.d.). *How do you select an experimental design?* Retrieved November 20, 2022, from NIST: https://www.itl.nist.gov/div898/handbook/pri/section3/pri33.htm

Prusa 3D. (2022, December 10). *Linear advance*. Retrieved from Help Prusa 3d: https://help.prusa3d.com/article/linear-advance_2252

Prusa3d. (2022). *Extrusion multiplier calibration*. Retrieved October 23, 2022, from https://help.prusa3d.com/article/extrusion-multiplier-calibration_2257

Prusa3D. (2022). *Stringing and oozing*. Retrieved October 23, 2022, from https://help.prusa3d.com/article/stringing-and-oozing_1805

SME. (2022, December 12). *Additive Manufacturing Glossary*. Retrieved from https://www.sme.org/technologies/additive-manufacturing-glossary/#:~:text=Additive%20manufacturing%20is%20a%20process,laid%20down%20in%20different%20shapes.

Sunon. (2022). *DC Brushless Fan & Blower.* Retrieved 12 30, 2022, from https://www.sunon.com/eu/MANAGE/Docs/PRODUCT/299/475/SUNON%20DC%20Brushless%20Fan%20&%20Blower(255-E).pdf

Voxeljet. (2022, 12 5). *Stereolithography(SLA) & 3D printing*. Retrieved from https://www.voxeljet.com/additive-manufacturing/3d-printing-processes/stereolithography/#:~:text=What%20is%20stereolithography%20(SLA)%3F,makers%20to%20larger%2C%20industrial%20systems.

Wütrich, M., Gubser, M., Elspass, W. J., & Jaeger, C. (2021, September 21). A Novel Slicing Strategy to Print Overhangs withoutSupport Material. *Applied Sciences*. doi:https://doi.org/10.3390/app11188760

Appendix A Time plan

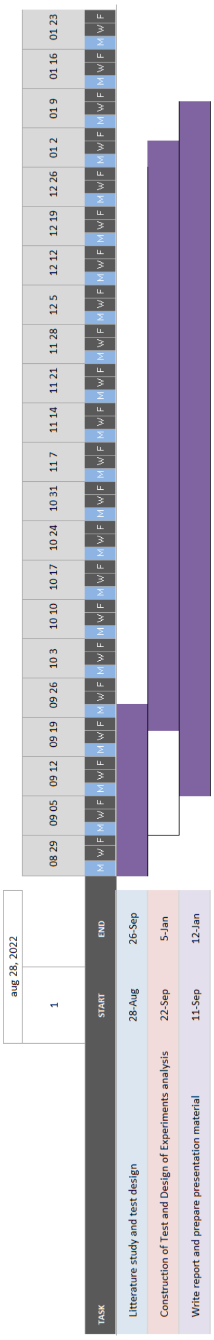

Figure A.1 The Performed activities. The start of the experiment construction was delayed due to delays in procuring parts for theprinter that was planned to be used.

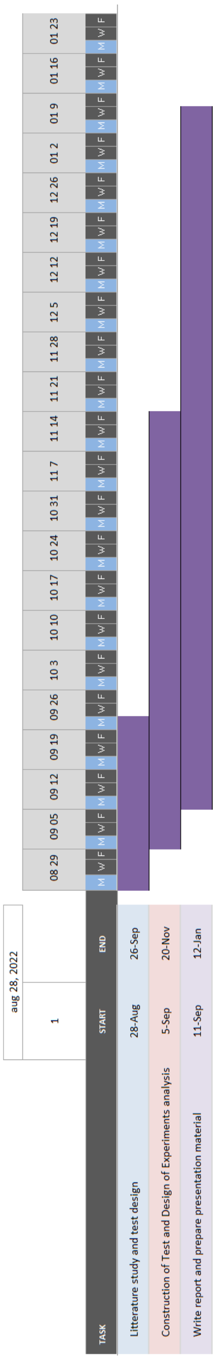

Figure A.2 The planned activities.

Appendix B Machine drawings

The following appendices will show the first show the original nozzle design and thereafter the newly designed ones used for experimentation in greater detail than was possible in the main text.

B.1 E3D Nozzle

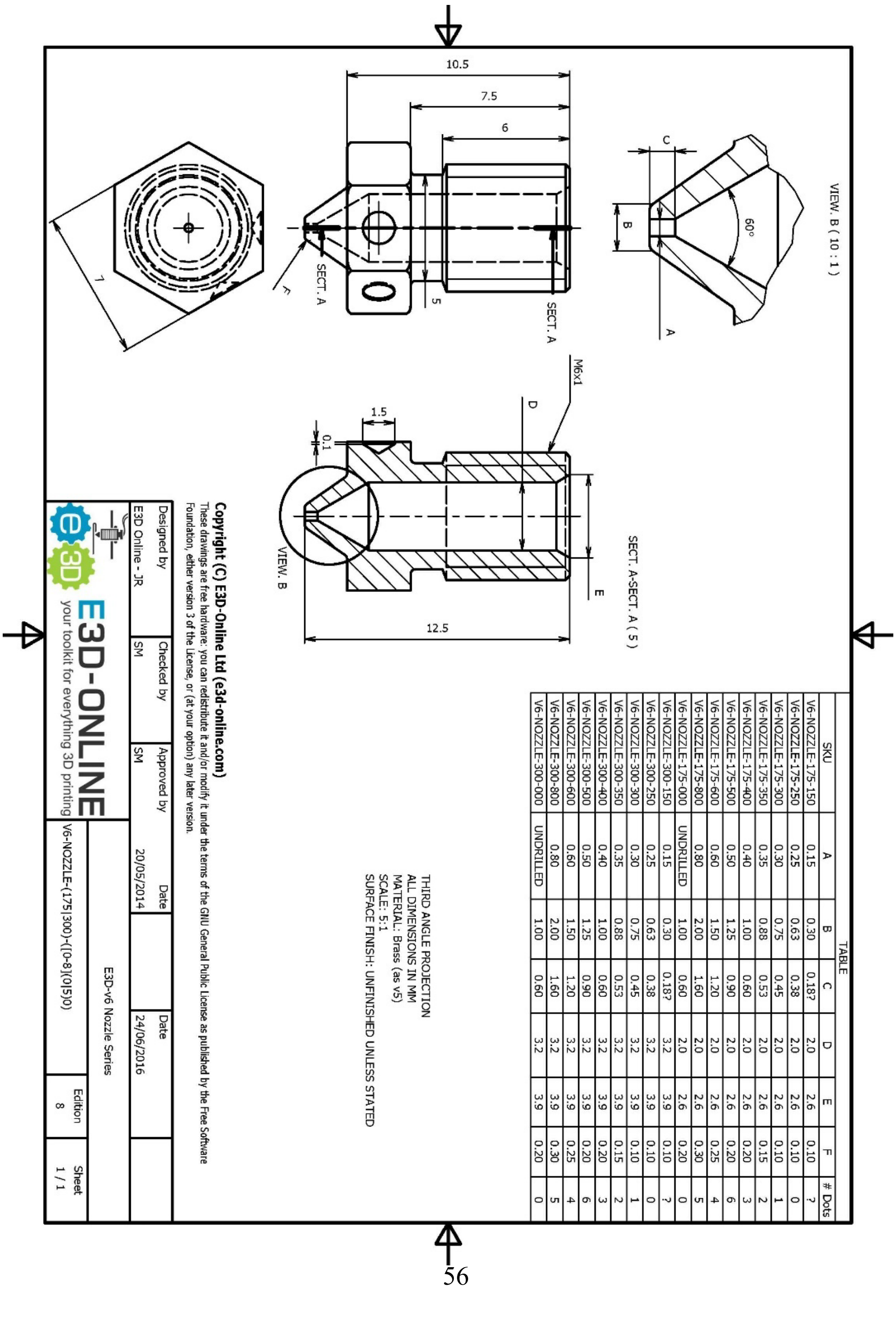

TABLE

SKU	A	B	C	D	E	F	# Dots
V6-NOZZLE-175-150	0.15	0.30	0.18?	2.0	2.6	0.10	?
V6-NOZZLE-175-250	0.25	0.63	0.38	2.0	2.6	0.10	0
V6-NOZZLE-175-300	0.30	0.75	0.45	2.0	2.6	0.10	1
V6-NOZZLE-175-350	0.35	0.88	0.53	2.0	2.6	0.15	2
V6-NOZZLE-175-400	0.40	1.00	0.60	2.0	2.6	0.20	3
V6-NOZZLE-175-500	0.50	1.25	0.90	2.0	2.6	0.20	6
V6-NOZZLE-175-600	0.60	1.50	1.20	2.0	2.6	0.25	4
V6-NOZZLE-175-800	0.80	2.00	1.60	2.0	2.6	0.30	5
V6-NOZZLE-175-000	UNDRILLED	1.00	0.60	2.0	2.6	0.20	0
V6-NOZZLE-300-150	0.15	0.30	0.18?	3.2	3.9	0.10	?
V6-NOZZLE-300-250	0.25	0.63	0.38	3.2	3.9	0.10	0
V6-NOZZLE-300-300	0.30	0.75	0.45	3.2	3.9	0.10	1
V6-NOZZLE-300-350	0.35	0.88	0.53	3.2	3.9	0.15	2
V6-NOZZLE-300-400	0.40	1.00	0.60	3.2	3.9	0.20	3
V6-NOZZLE-300-500	0.50	1.25	0.90	3.2	3.9	0.20	6
V6-NOZZLE-300-600	0.60	1.50	1.20	3.2	3.9	0.25	4
V6-NOZZLE-300-800	0.80	2.00	1.60	3.2	3.9	0.30	5
V6-NOZZLE-300-000	UNDRILLED	1.00	0.60	3.2	3.9	0.20	0

B.2 Nozzle A1 – Extended

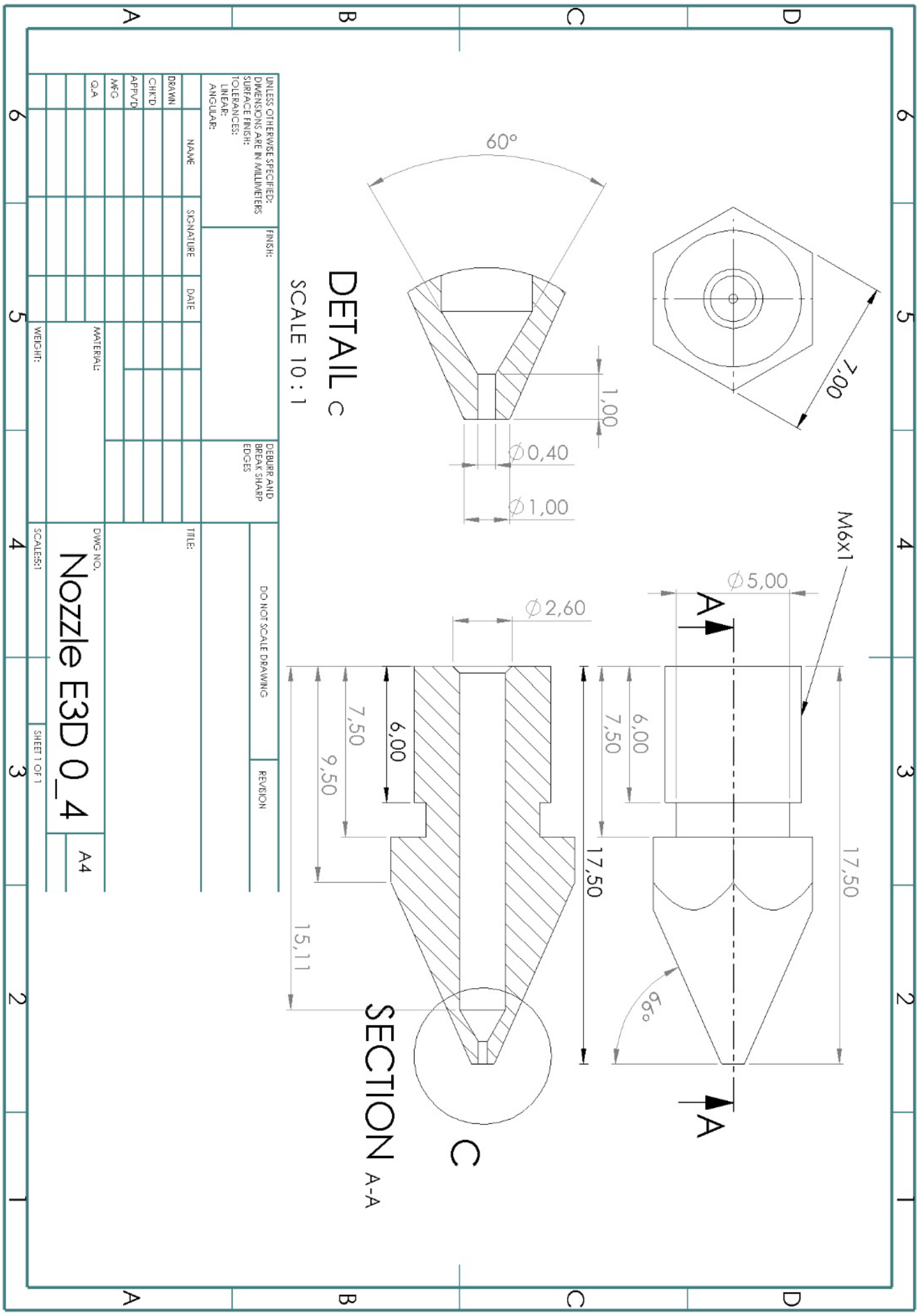

B.3 Nozzle A2 – Extended and with 30° tip angle

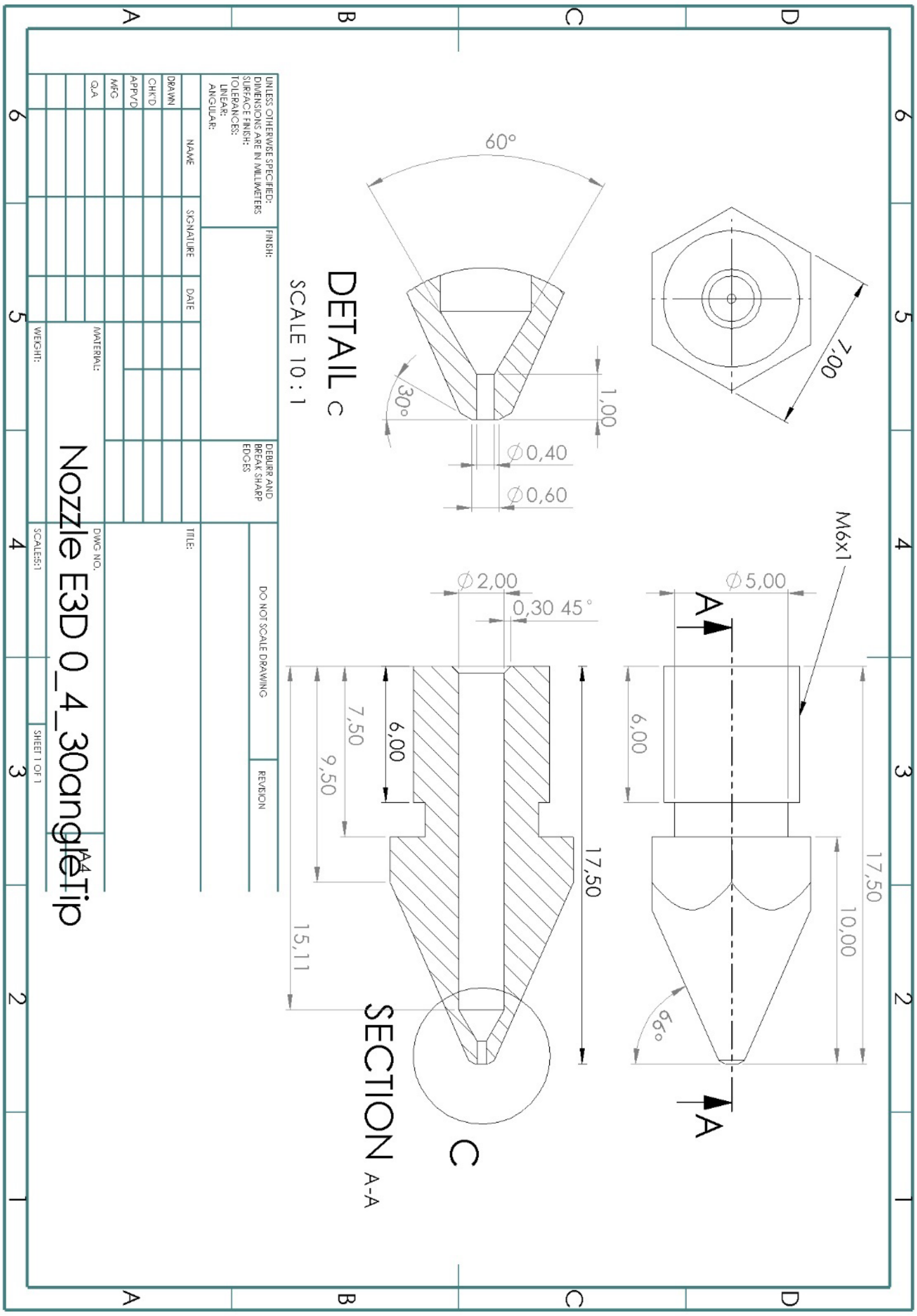

B.4 Height sensor retraction mechanism

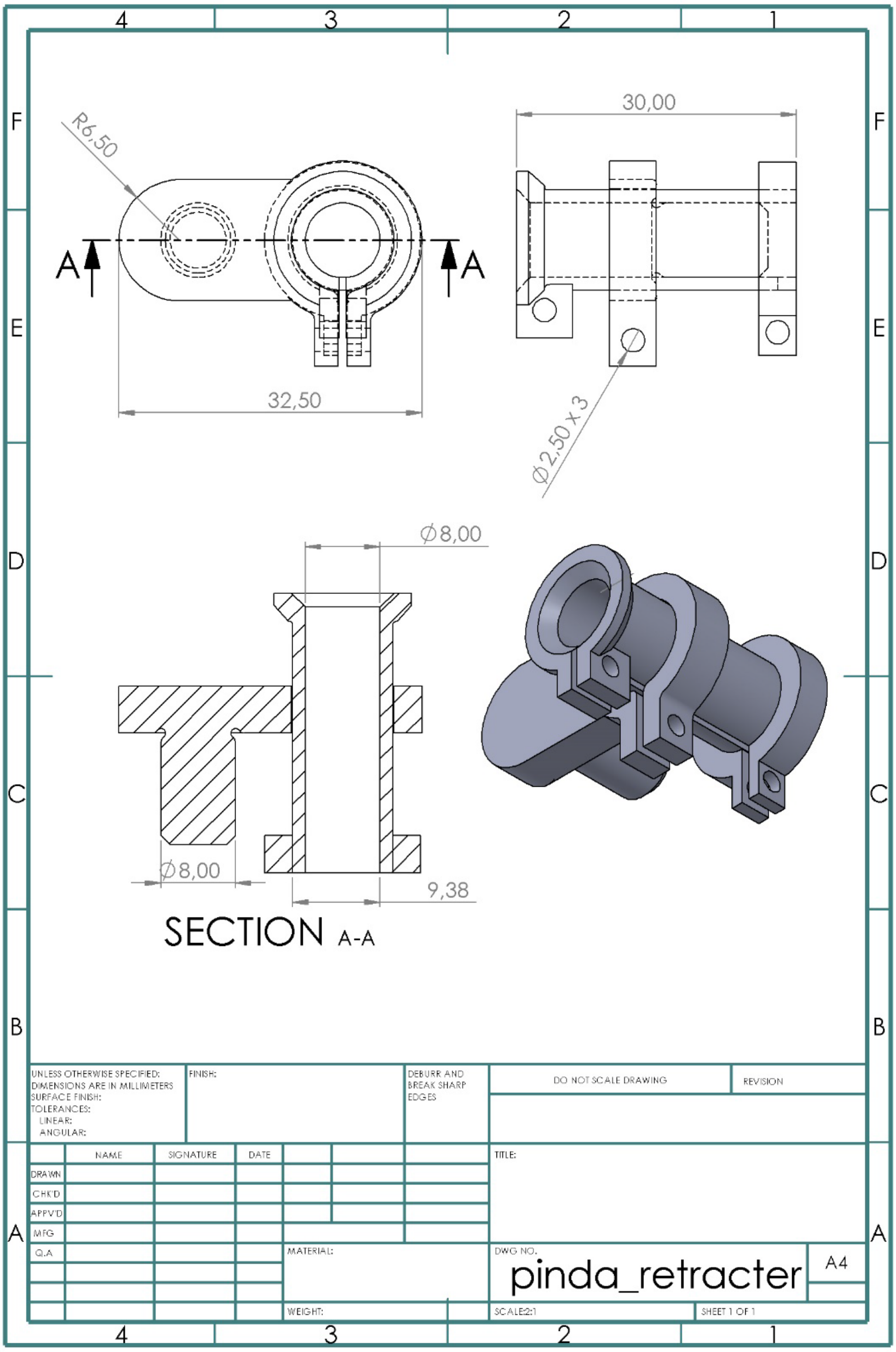

B.5 Fixture for attaching camera to picture box